

ELASTODYNAMIC ANALYSIS OF A CAM-MODULATED MECHANISM

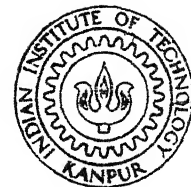
by

AVIJIT ROY

ME
1985
M

ME/1985/m

R 812e



Roy
Ela

DEPARTMENT OF MECHANICAL ENGINEERING
INDIAN INSTITUTE OF TECHNOLOGY, KANPUR
MAY, 1985

ELASTODYNAMIC ANALYSIS OF A CAM-MODULATED MECHANISM

A Thesis Submitted
In Partial Fulfilment of the Requirements
for the Degree of
MASTER OF TECHNOLOGY

by
AVIJIT ROY

to the

DEPARTMENT OF MECHANICAL ENGINEERING
INDIAN INSTITUTE OF TECHNOLOGY, KANPUR
MAY, 1985

10 JUN 1985

WIT SIMP JR
87573

ME-1985-M-ROY-ELA

9/5/85
CERTIFICATE

Certified that the work presented in this thesis entitled 'Elastodynamic Deflection Analysis of a Cam-modulated Mechanism' by Sri Avijit Roy, has been carried out under our supervision and has not been submitted elsewhere for a degree.

A. Ghosh

A. Ghosh
Professor
Dept. of Mechanical Engineering
Indian Institute of Technology
Kanpur

S.G. Dhande

S.G. Dhande
Asst. Professor
Dept. of Mechanical Engineering
Indian Institute of Technology
Kanpur

Date: May 5, 1985

12/5/85
Avijit Roy
Kanpur

ACKNOWLEDGEMENT

I acknowledge with deep gratitude the invaluable help, able guidance and constant encouragement provided by my thesis advisors Dr. Amitava Ghosh and Dr. S.G. Dhande without which the thesis work could not reach completion.

I wish to express my thanks to my friends, specially 'B-middle' who readily extended their help from time to time.

Thanks are due to Mr. S.N. Pradhan who carefully typed the manuscript.

Avijit Roy

CONTENTS

		Page
ABSTRACT		
LIST OF FIGURES		
LIST OF SYMBOLS		
CHAPTER I	INTRODUCTION	
1.1	Elastodynamics of Planar	
	Mechanisms	1
1.2	Valve Train in Automotive	
	Engines	5
1.3	Literature Survey	7
1.4	Objective of the Present work	11
1.5	Limitations	13
CHAPTER 2	ELASTODYNAMIC MODELLING	
	OF VALVE TRAIN	
2.1	Kinematics	15
2.1.1	Rigid Body Displacement	18
2.2	Elastodynamic Modelling of Cam-pair	20
2.3	Elastodynamic Modelling of Linkage	26
2.3.1	Element Property Matrices	27
2.3.2	System Model	30
2.4	Analysis Approach	
2.4.1	Methodology	40
2.4.2	Solution Procedure	42
2.4.3	Force Vector	47

			Page
CHAPTER	III	COMPUTER PROGRAMS	50
CHAPTER	IV	COMPUTATIONAL WORK	54
	4.1	Numerical Example	54
	4.2	Results and Discussions	56
CHAPTER	V	CONCLUSIONS	
	5.1	Technical Summary	67
	5.2	Recommendations	70
APPENDICES			
APPENDIX I		Determination of Area Moment of Inertia of Cam Profile	71
APPENDIX II		Derivation of Cam Stiffness	73
APPENDIX III		Determination of Eigen-Value and Eigen-Vector.	75
REFERENCES			

ABSTRACT

In the present work, a methodology for Elastodynamic analysis of the valve train mechanism has been presented. The valve train mechanism is essentially a cam-modulated linkage. This mechanism is widely used in I.C. engines and forms an important subsystem. A model for the elastodynamic analysis of a higher pair has been proposed. Using this proposed model for the higher pair and the conventional models for lower pairs of the valve train mechanism, it has been shown as to how to obtain the error between the cam command and follower response. The error is a function of the input speed and this dependence has been studied. A computer program based on the methodology proposed has been developed, tested. Using this programme, it is possible to study the influence of various design parameter on the performance of the valve train mechanism.

LIST OF FIGURES

Figure		Page
1.1	- Overhead Valve in an Automotive Engine	6
2.1	- A Radial Cam and Translating Roller Follower	17
2.2	- Instantaneous Kinematic Equivalent Linkage	17
2.3	- Cam Under Load P	24
2.4	- Tapered Cantilever Beam	24
2.5	- Two Cylinders at Contact	24
2.6	- Element Oriented Element Co-ordinates	28
2.7	- System Oriented Element Co-ordinates	28
2.8	- Idealised Model of the Valve Train Showing System Coordinate	32
2.9a -2.9f	- Individual Element Co-ordinates	34
4.1	- Cam Profile for the Numerical Example	55
4.2	- Valve End Displacement Versus Cam Rotation	57
4.3	- Cam Characteristica Curves	59
4.4,4.5	- Variation of Deflection at Various Operating Speed	61,62
4.6	- Deflection at Valve end based on Rigid Body Forces Only	64
4.7	- Variation of First Natural Frequency with Cam Position	65

LIST OF SYMBOLS

A	-	Area of Cross-Section of an element
I	-	Second moment of inertia of the cross-section also identity matrix
L	-	Length of an element
E	-	Young's Modulus
γ	-	Density of material
$[m], [k]$	-	Element mass and stiffness matrices in element (local) coordinate respectively
$[\bar{m}], [\bar{k}]$	-	Element mass and stiffness matrices in system co-ordinate respectively
$[M], [K]$	-	System mass and stiffness matrices respectively
$[C]$	-	System damping matrix
u	-	Element displacement vector
U	-	Global displacement vector
F	-	Force vector
I_c	-	Mass moment of inertia of cam about centre of rotation O
I_{cr}	-	Mass moment of inertia of crank about centre of rotation O
r_1	-	Crank length in equivalent linkage
r_2	-	Connecting rod length in equivalent linkage

- K_b - Stiffness of Cam (crank)
- K_H - Stiffness of connecting rod
- ϕ - Modal matrix
- ω - Natural frequency of the system
- Vector containing eigen values
- i - Damping ratio corresponding to i -th normal mode
- η - Displacement vector in normal co-ordinate system

CHAPTER I

INTRODUCTION

1.1 ELASTODYNAMICS OF PLANAR MECHANISM:

The kinematic analysis and synthesis of any planar mechanism has become a powerful design tool for engineers. The technique of kinematic analysis, however, suffers from a major drawback. This is the 'rigidity' assumption which prevails throughout the literature with few notable exceptions. Mechanisms consisting of gears, links, sliders etc. in real world application are not at all rigid. They are sensitive to elastic deflections when they are subjected to high static or dynamic forces. The dynamic forces play an insignificant role when the machine or mechanism is operated at low speed range. Consequently, a designer does not need to concern himself about the inherent elasticity present within the system. The idealization of the mechanism as consisting of 'purely rigid members' in the analysis or design process does yield results within the designers satisfactory level as long as the operating speed is kept low and so long the accuracy required in the relationship of input and output is not very high.

The situation turns out to be significantly different in the case when the same mechanism is operated at higher speeds. Dynamic forces increase with the increase of acceleration of different members. For sufficiently larger speeds, these force may even play a predominant role. Thus the rigidity assumption, generates inaccurate analysis and synthesis which may lead to improper functioning of the machine and eventually failure of the members particularly at high speeds. A machine or mechanism which is kinematically adequate at slow speeds may have sufficiently different motion at high speed so that it can no longer perform its intended function. Apart from this, in high speed mechanisms, the chances of the mechanism being subjected to resonant condition is also quite high.

Within the domain of present day automation, machineries are required to operate at higher speeds and at minimum power. The accuracy requirements in such machines are also showing an increasing trend. Elastic deflections which are the consequences of increased speeds and loads may cause inaccuracies of position in addition to noise and fatigue.

From the above facts, it becomes thus apparent that the usual design or analysis procedures may not yield satisfactory results. Need for newer methods and advanced

techniques was felt for analysis and design of mechanisms with elastic members. Literature has already recognized a considerable amount of research work in this area. The outcome of these efforts has made a way to a newer and advanced method, Kineto-elastodynamics, an analysis and synthesis technique which can take care of kinematics as well as finite rigidity of the members. It has become an efficient and powerful tool to the designers.

Kineto-elastodynamics in general, is the examination of displacement, velocities, accelerations, stresses, strains etc. of a moving elastic mechanism. Effects of elastic deformations upon the inertia forces are included in the analysis. Whereas, the Elastodynamic analysis of a mechanism defines the same thing as the previous one except that the inertia forces are calculated by assuming the members rigid. Both the methods take into account the mass distribution of the links. The principles and concepts of finite element method used in structural dynamic analysis is greatly utilised in performing the kineto-elastodynamic analysis of any planar mechanism.

Over the past decade, since its origin, lot of improvements have been carried out towards the generalisation of KED analysis technique for studying lower pair planar

mechanisms. Most of the researchers in this field have developed methods or improved over the previous methods specific application to the planer four bar mechanisms (e.g., 4-bar slider-crank mechanism, crank-rocker mechanism 4-bar path generating mechanism etc.). Their applications were limited to planer lower-pair mechanism. On the other hand, higher-pair mechanisms did not get much attention on the employment of the analysis method.

Cam-modulated mechanisms are noteworthy examples of higher-pair mechanism. In the construction of modern machines their importance are obvious. They find their use immensely in automotive engines, aircraft engines, textile machineries, automatic machines etc. Overhead valve-train linkage used in automotive engine is one of the simplest example of a cam-modulated linkage. In the context of smooth operation, efficient performance of the engine the valve-train mechanism gets due importance. The overall performance of mechanism depends largely on the proper design of the cam profile. Hence, a comprehensive and accurate analysis compared to the previously used ones of the complete mechanism is essential which helps in achieving better performance.

1.2 OVERHEAD VALVE-TRAIN IN AUTOMOTIVE ENGINE :

A typical cam-driven overhead valve-train linkage used in automotive engine is shown in Fig. 1.1. This mechanism consists of a pushrod, rocker arm, valve, valve-spring apart from the cam and follower. The movement of the valve is governed by the cam profile. The valve controls the flow of air fuel mixture into the engine cylinder. The amount of air fuel mixture getting into the cylinder determines to some extent the thermodynamic efficiency of the engine, thus the importance of the proper valve movement.

In almost all the automotive engines the response of the follower end that is of the valve end does not remain same as that of machined on the cam profile, (i.e., cam command). This is inevitable particularly at higher speed. The discrepancy in cam command and follower response is a result of the high flexibility or elasticity of the follower train and the magnitude of dynamic forces prevalent in the mechanism as a consequence of higher speed. In the context of accurate design of cam profile correct estimation of the difference between cam command and response is essential.

Thus a need is felt to investigate the discrepancy through comprehensive analysis utilising the newer methods, like elastodynamics.

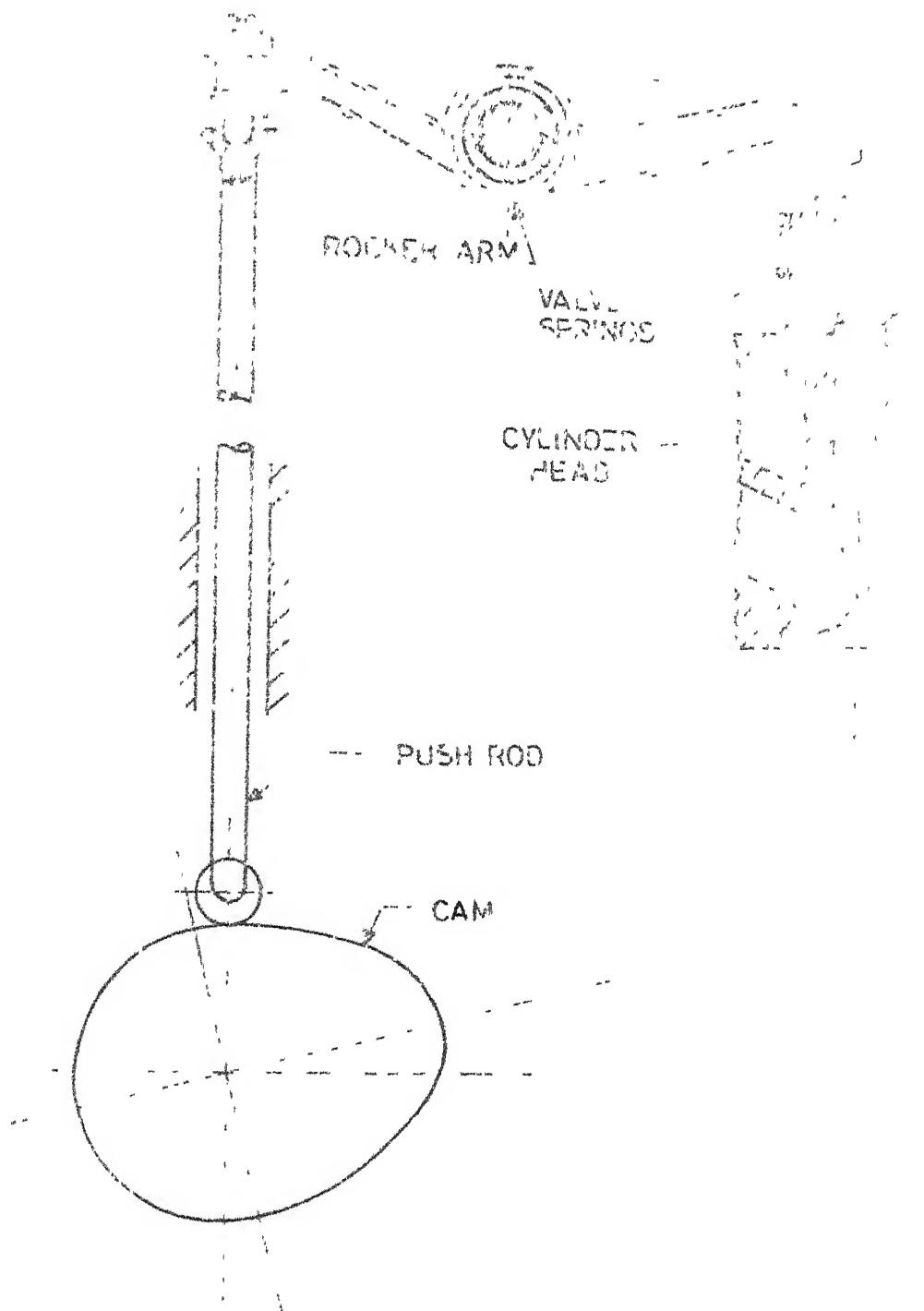


FIG.1.1 OVERHEAD VALVE IN AN AUTOMOTIVE ENGINE

1.3 LITERATURE REVIEW:

During the earlier stage the works that were conducted, the researcher analysed the mechanisms based on the mathematical model with only one elastic member [10]. For instance, in 1965, Neubauer, Cohen and Hall [10] analysed a slider-crank mechanism containing an elastic coupler rod. In the next decade the analysis method developed, assumed either most or all the members were elastic.

Winfrey [21] performed an analysis of longitudinal, transverse and torsional displacements of a general mechanism. He was the first to use finite element method in the area of mechanism analysis. For each planer link he defined 6 elastic coordinates (3 at each end of the link) and 3 rigid body coordinates.

Erdman, Sandor and Oakberg [5] developed a general method for kineto-elastodynamic analysis and synthesis of planer mechanism. They incorporated flexibility approach of the finite element method in the analysis. The input crank is considered to behave like a cantilever beam thus converting the mechanism to ' structure ' and a system flexibility matrix is developed. A Kineto-elastodynamic stretch rotation operator (KEDSRO) describing the elastic motion of a single point is used. This finds out the

deflections by an iterative procedure, which starts from rigid body inertia forces.

In 1973, Iman, Sandor and Kramer [7] came up with a method of deflection analysis of general planar single and multi-loop linkages. The extension of permutation vector is used to carry out the assembly of elements. This method numbers the system co-ordinates automatically and it does not offer any special advantages in the sense that system coordinates are less in number in case of a mechanism. They also use for the first time the rate of change of eigenvalue and eigenvectors in mechanism analysis in an effort to reduce the computational time. A reduction by a factor of 3 is found by them. The force vector is calculated by multiplying the system mass matrix with the negative of the acceleration (rigid body) vector and assumed to remain constant during each interval. Input crank is considered as a cantilever beam since no system co-ordinate is defined at the support end. A method of computing dynamic stresses is also discussed in this paper.

Midha, Erdman and Frohrib [8] described general procedures for studying high speed elastic linkages using finite element displacement method of structural analysis technique. The expressions for nodal displacements,

accelerations etc. include the terms coupling the rigid-body and elastic motions. The effects of additional acceleration terms are neglected in the final form of these expressions. The input crank here also is modeled as a cantilever beam.

Winfrey [19] reported a method for dynamic analysis of flexible mechanism by reduction of co-ordinates. The total number of system co-ordinates is reduced to only one coordinate at the point of design interest. Thus a considerable amount of computational time is saved by solving a single degree of freedom system of the same elastic mechanism. Results he obtained, as expected differs from that of the complete solution.

In his analysis method Nath [9] treated each link with no. of subdivisions for accurate modelling as compared to the previous works. A new and efficient technique is developed to eliminate the rigid body degrees of freedom instead of taking the input link as a cantilever beam. While deriving the element property matrices he takes into account the effect of rotary inertia and shear. To construct the system matrices code-system of assembly is adopted to incorporate various mechanism conditions.

Erdman and Sandor [6] presented a review of the state of the art and trends in kineto-elastodynamics. The

nomenclature used in KED is consolidated in this work in organised form.

Winfrey, Anderson and Gnilka [20] studied an elastic machinery with clearance. The analysis approach is presented with elastic model citing the example of a cam-driven automotive overhead valve-train linkage. The elastic model of the follower train is formulated using the finite element technique for structural analysis. The entire analysis process assumes constant geometry of the mechanism. He models the component parts as simple prismatic elements. The problem of impact is also investigated in this work taking help of the elastic model prepared for the follower train.

Previous works as discussed in the above-mentioned literature contributed towards the establishment of the foundation of the kineto-elastodynamic technique. Their applications are confined around primitive four-bar mechanism and also to multi-loop linkages in few instances. From the point of view of applying the kineto-elastodynamic analysis to cam-activated mechanism almost no prior effort is made. Of course, works have been carried out in the past decades by numerous researchers to model a cam-follower system. Many works have been published on the study of dynamic response of different types cam-follower system with the

aid of conventional single-degree or multiple degree of freedom mass, spring, damper representation.

Barken [2] dynamically modeled an automotive overhead valve train using the lumped mass approach. Initially he forms a multidegree of freedom model containing massless springs and rigid masses. Then he reduces it to a single-degree of freedom model and solves to find dynamic response of the system. Stoddart [14] introduced a new method, namely (Polydyne cam design) to design a cam profile for an automotive engine accounting the elasticity of the follower train. In the present work an attempt is made to estimate the elastic deflection of a cam-actuated linkage exploiting elastodynamic technique.

1.4 OBJECTIVE OF THE PRESENT WORK :

The analysis or synthesis of a cam-follower system performed by numerous workers in the previous years utilizing lumped mass approach and mass-spring damper model suffers from few drawbacks. These can be stated as lack of generality in approach, inaccuracy incurred in calculating deflections etc. The concept of finite element method with its versatility may be used to eliminate the above shortcomings in the context of analysis of cam mechanism.

Analyzing a cam-actuated follower train with the aid of elastodynamic technique possess certain difficulties. Being a higher pair the cam-follower cannot directly be fitted into the methodology of elastodynamic modelling technique for the purpose of modelling them.

Unlike the links in a lower-pair mechanism the known structural beam elements cannot possibly be applied to model the cam-follower pair directly. Obviously, it becomes necessary to obtain an appropriate equivalent model of the cam-follower pair which when combined with the rest of the follower linkage enables one to exploit the potentiality of elasto-dynamic analysis technique and eventually to perform the analysis.

The objective of the present work may be narrated as follows:

(i) an attempt will be made to represent a cam-follower pair to its corresponding lower-pair elements which can approximately (if not accurately) becomes equivalent as far as the elastic and dynamic behaviour of the actual system is concerned. The lower-pair equivalent model will also be made kinematically equivalent. It becomes apparent that the finite rigidity of the cam body comes into picture and in a way forms a part of total system stiffness.

(ii) to formulate the system model in terms of system co-ordinates in order to perform the deflection analysis. The elastic behaviour of the system will be examined at various operating speed.

The analysis will be carried out for an automotive overhead valve-train linkage which is a cam-modulated higher-pair mechanism. A radial cam with translating roller follower is chosen for the sake of simplicity in illustrating the analysis procedure throughout.

1.5 LIMITATIONS:

The analysis approach that is followed has got few limitations and assumptions.

In formulating the system model for the complete valve train the input crank in the equivalent mechanism is modeled as a cantilever beam. This bypasses the purpose of eliminating the rigid body degrees of freedom and the mechanism is not analysed under actual boundary conditions.

The force vector in solving the system equations of motion consists of the contribution from inertia forces arising due to gross or rigid body motion of the mechanism in the course of motion. This does not take into account the actual distribution of the rigid body inertia forces over the

lengths of the element. Any external forces if present, is also included in force vector.

The assumptions that are taken are :

(i) the input angular velocity is assumed to remain constant.

(ii) the rigid body motion and elastic vibrations are seperable.

(iii)the deflections are small so that the linear theory can be applied throughout.

(iv)the effects of clearances, tolerances are neglected.

CHAPTER II

ELASTODYNAMIC MODELLING OF VALVE TRAIN

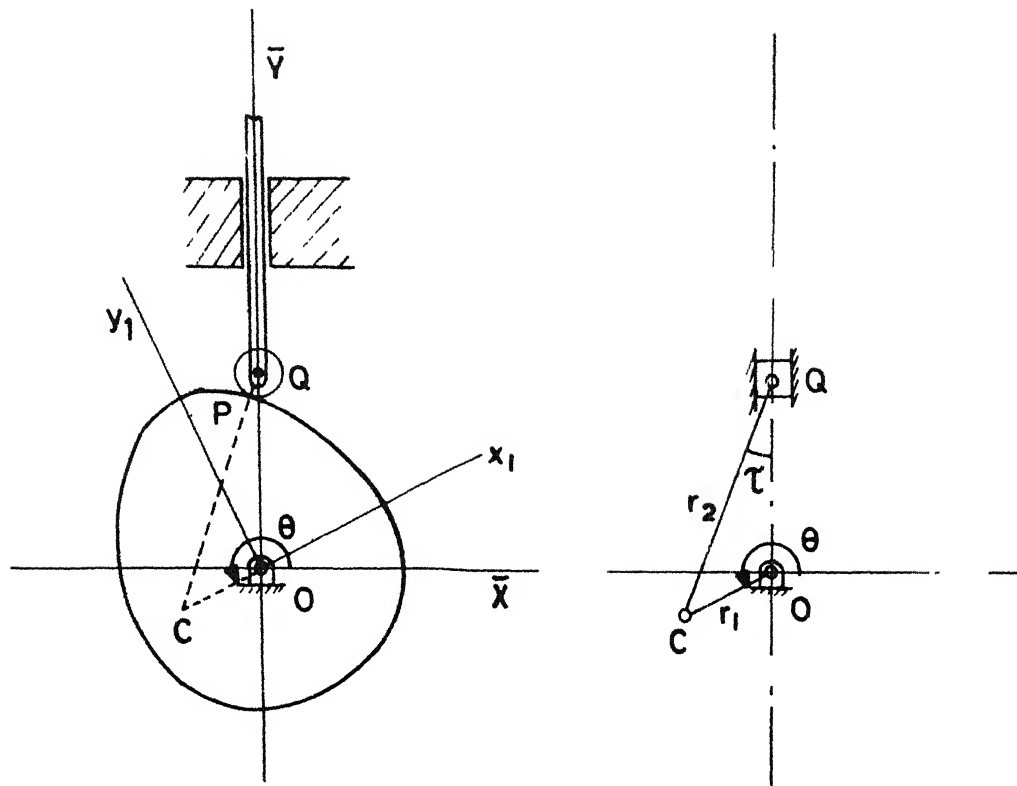
2.1 KINEMATICS :

As indicated in the Chapter I the type of cam-follower pair that is being considered in the present work a radial cam with translating roller follower. In order to carry out the elasto-dynamic analysis of the entire mechanism as a first step it is necessary to model the cam-follower pair first. Most of the lower pair mechanisms (like, slider-crank, crank-rocker etc.) are comprised of binary links mainly and of ternary links in some cases. Analysing those mechanisms, a binary link can very simply be represented by a structural beam element. The ternary link can also be represented by attaching appropriate degrees of freedom at the nodes. But a cam-follower pair which is a higher-pair (that means the nature of contact between them is either point or st.line) cannot directly be modeled using simple beam elements. Cam is basically a disc and followers also do appear in various forms.

Thus difficulties are encountered in modelling the cam follower pair. But a higher pair can also be

converted to a lower pair such that the latter becomes instantaneously equivalent kinematically to the former one. That is at the point of contact the kinematic quantities like displacements, velocity, and accelerations are all identical instantaneously for both the higher-pair and lower pair. Similarly, a cam-roller follower can always be transformed into an equivalent lower pair mechanism to obtain a instantaneous kinematic equivalency at the point of contact. Having made the kinematic equivalency by converting to a lower-pair structure it can be possible now to start with analysis if the dynamic equivalency of the two system is achieved. In the following section of this chapter (section 2.2) an attempt is made to obtain an equivalent elasto-dynamic model of the cam-pair at least approximately.

Let us consider a radial cam and a translating roller follower (see Fig. 2.1) . The direction of the follower motion is coinciding with the \bar{Y} -axis of the cam. $\bar{X}-\bar{Y}$ is the fixed axis and $x_1 - y_1$ is a moving co-ordinate frame embedded on the cam profile. The follower displacement is dictated by the characteristic shape of the cam profile . Let P be the point of contact at the instant shown when the $x_1 - y_1$ frame inclines say, at some angle ϕ with $\bar{X}-\bar{Y}$. To create an instantaneously equivalent lower-pair mechanism the



A RADIAL CAM AND TRANSLATING
ROLLER FOLLOWER .

FIG. 2.1

INSTANTANEOUS KINEMATIC
EQUIVALENT LINKAGE

FIG. 2.2

centre of curvature C of the cam-profile is located. For the roller follower the same is the point Q.

It can be shown that [11] OCPQ which represents a slider-crank mechanism (see Fig. 2.1,2.2) is equivalent instantaneous 4 bar mechanism to the situation under consideration . The follower motion and the slider motion are identical for the instant considered. Distance PQ for a roller follower always remains constant. The location C, thus the distance OC and CP varies with the cam profile. A harmonic cam with constant radius of curvature can be permanently represented by a slider-crank mechanism with constant link lengths. With arbitrary cam profile the link lengths OC and CQ changes when the actual cam rotate through any definite angle.

2.1.1 RIGID BODY DISPLACEMENT :

When a mechanism undergoes rigid body displacement no elasticity or flexibility comes into picture. Members are assumed purely rigid. The functioning of the overhead valve train (see Fig.1.1) is as follows. The pushrod is constrained to move only along the guide. The rotation of the cam causes the pushrod move up and down depending on nature of the cam profile. During the rise period (when the valve opens) the

pushrod is raised up by the cam action. This causes one end of the rocker arm to move up. The valve side end of the rocker arm pushes down on the valve stem-causing the valve to move down or open. The valve takes the close position by the spring action when the cam passes through return period. The displacement at the cam end is faithfully transmitted to the valve end multiplied by a-factor (lever ratio).

Let the displacement at the cam end be d_c , measured from a datum (say the base circle), when the cam has turned through an angle of ϕ degree. At this instant d_c is found from the profile curve. d_c can also be obtained from the equivalent linkage. The valve-end displacement is given as

$$d_v = d_c \times c, \quad \dots \dots \quad (2.1)$$

where c - rocker arm lever ratio

d_v - valve end displacement

assuming small rigid body displacement.

From the Fig. 2.2 , the following expression for d_c is written, valid for the instant shown

$$d_c = r_2 \sin \gamma + r_1 \sin \theta - R_b \quad \dots \dots \quad (2.2)$$

where,

r_2 - connecting rod length

r_1 - crank length

γ -
 θ - shown in Fig. 2.2

R_b - base circle radius

2.2 ELASTO-DYNAMIC MODELLING OF THE CAM-FOLLOWER PAIR :

In the previous section of this chapter a kinematically equivalent lower-pair mechanism has been found out which is a slider crank 4-bar linkage. In general the two link lengths(Fig. 2.2) r_1 (of the crank) and r_2 (of the connecting rod) are expected to vary because the centre of curvature, is not going to remain fixed. Kinematic equivalence assumes links to be rigid. The aim of this section is to form a equivalent model of the cam-follower system for the purpose of elasto-dynamic analysis. Basically, the task of modelling finally comes down to modelling a lower-pair system incorporating appropriately the elastic and dynamic behaviour of the actual system.

It is observed (Fig. 2.1) that in the actual system the cam is purely rotating body, rotating about the axis passing through O and perpendicular to the plane of the paper. The crank in the equivalent slider-crank mechanism is

purely rotating member. The 'crank' and the cam are revolving about the same centre of rotation. From the fact it can be assumed that the 'crank' and the cam are maintaining rotational equivalency if their mass moment of inertia are equalised about the same centre of rotation.

In other words, it is meant that the 'crank' is behaving like a 'rod like cam'. Equating mass moment of inertia of the two purely rotating body both are moving at same angular velocity, implies their dynamic equivalency. Thus the crank of the kinematically equivalent mechanism can have some mass.

Let the mass moment of inertia of the actual cam about the centre of rotation O = I_c and

I_{cr} = mass moment of inertia of the crank about O.

Consider the crank is having uniform circular cross-section area of radius r. If the cam profile is known completely the it's mass moment of inertia can be computed. For a thin disc/ plate of uniform thickness 't' and made up of a homogeneous material of density ' γ ' the polar moment of inertia I_{cc}' is given by [3].

$$I_c = I_{cc}',_{\text{mass}} = \gamma t \cdot J_{c, \text{area}} \quad \dots (2.3)$$

where,

$J_{c, \text{area}}$ = polar moment of inertia of area of the plate about point O.

$J_{c, \text{area}}$ of a given cam profile can be computed numerically (discussed in Appendix I). Crank is considered as a circular cylinder. Mass moment of inertia of it about O is expressed as [3]

$$I_{cr} = \frac{m}{12} (3r^2 + 4r_1^2) \quad \dots \dots (2.4)$$

where,

m = mass of the crank,

r = radius of cylinder

Equating (2.3) and (2.4)

$$\begin{aligned} I_c &= \frac{m}{12} (3r^2 + 4r_1^2) \quad \dots \dots (2.5) \\ &= \frac{m}{12} (3 \frac{m}{K} + 4r_1^2) \end{aligned}$$

where,

$$K = \pi \gamma r_1$$

$$\text{or, } 12KI_c = \frac{3m^2}{K} + 4Kr_1^2 \quad m \quad \dots \dots (2.5a)$$

The equation (2.5a) is solved for unknown m as follows,

$$m_{1,2} = \frac{-4r_1^2 K \pm \sqrt{(r_1^2 K)^2 + 9KI_c}}{6} \quad \dots \dots (2.6)$$

$$\text{Feasible value of } m = \frac{-4r_1^2 K + 4\sqrt{(r_1^2 K)^2 + 9K I_c}}{6} \quad \dots \dots (2.7)$$

Though in the actual system the body of cam has got very high stiffness compared to the other member in the mechanism. An estimation of this can be made approximately so that the 'crank' can be made to possess finite amount of bending stiffness. The cam is assumed to be a cantilever of varying cross-section (see Fig. 2.3, 2.4). Under the load P the maximum deflection can be found as

$$\delta = \frac{P}{\frac{2}{3} E \cdot t / \frac{1}{c^3} \left[\ln\left(\frac{b}{a}\right) - \left(1 - \frac{a}{b}\right) + \frac{1}{2} \left(1 - \frac{a^2}{b^2}\right) \right]} \quad \dots \dots (2.8)$$

(see appendix II)

where,

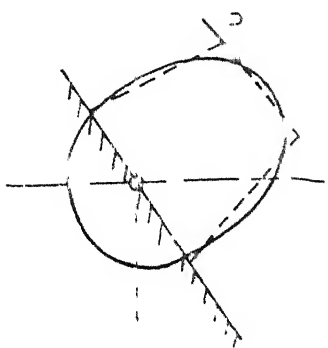
t = uniform thickness of the cam

$$c = \left(\frac{b-a}{L}\right)$$

From this expression the stiffness K_b is calculated

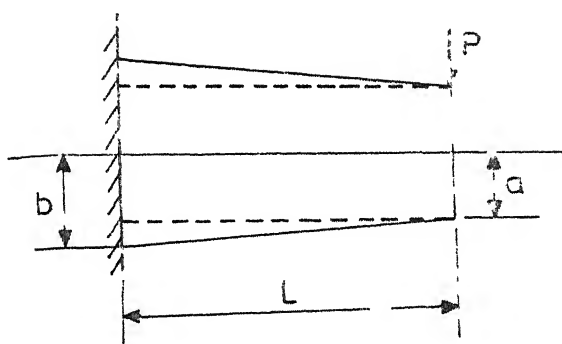
$$\text{as } K_b = \frac{2}{3} E \cdot t / \frac{1}{c^3} \left[\ln\left(\frac{b}{a}\right) - \left(1 - \frac{a}{b}\right) + \frac{1}{2} \left(1 - \frac{a^2}{b^2}\right) \right] \quad \dots \dots (2.9)$$

The connecting rod of the equivalent linkage is assumed massless. Since the actual cam and the crank are



CAM UNDER LOAD P

FIG. 2.3



TAPERED CANTILEVER BEAM

FIG. 2.4

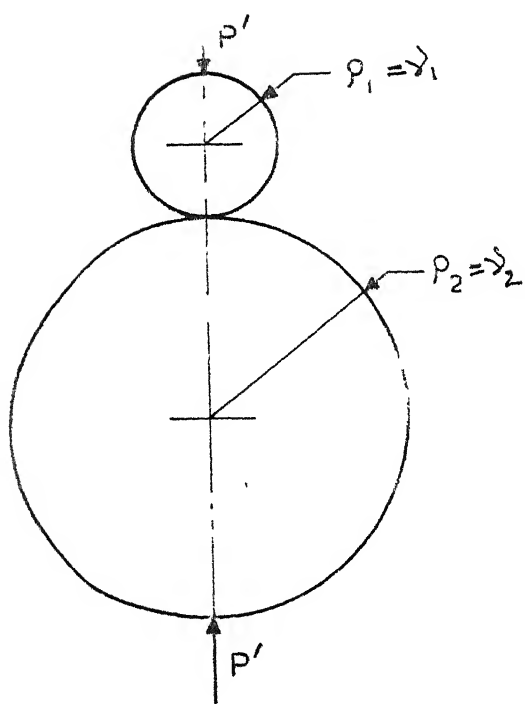


FIG. 2.5 TWO CYLINDERS AT CONTACT

made rotationally equivalent and the cam's counterpart mass in the crank is assigned, the connecting rod can be taken as massless. But it is permitted to deflect elastically only in its longitudinal direction. The stiffness of this link can be attributed due to Hertzian contactness at the cam-follower interface.

In actual cam-follower system a cylinder to cylinder contact is considered (see Fig. 2.5) [4].

The maximum normal stress σ_{\max} is given as

$$\sigma_{\max} = .564 \left[\frac{P' \frac{(\gamma_1 + \gamma_2)}{\gamma_1 \gamma_2}}{\frac{1 - \mu_1^2}{E_1} + \frac{1 - \mu_2^2}{E_2}} \right]^{1/2} \quad \dots (2.10)$$

where, E_1, μ_1 = Young's modulus and Poissons ratio for the body 1 (roller) respectively

Similarly E_2, μ_2 for the body 2 (cam).

Taking similar materials $E_1 = E_2 = E$ and $\mu_1 = \mu_2 = \mu$ expression (2.10) takes the form as in (2.11)

$$\sigma_{\max} = .564 \left[\frac{P' \left(\frac{\gamma_1 + \gamma_2}{\gamma_1 + \gamma_2} \right)}{2(1 - \mu^2)} \right]^{1/2} \quad \dots (2.11)$$

The stiffness K_H assigned to the connecting rod computed as

$$K_H = \frac{1}{.564 \left[\frac{\gamma}{2(1-\mu^2)} \right]^{1/2} \frac{1}{\sqrt{E}} \gamma_1} \quad \dots \dots (2.12)$$

$$\gamma = \frac{\gamma_1 + \gamma_2}{\gamma_1 \gamma_2}$$

It is to be noted that for every geometric configuration of the cam the γ_2 , and consequently K_H values are going to change.

Thus, an estimation of the mass and stiffness of the two links in the original kinematically equivalent linkage could be made, and an approximate model for the actual cam follower system is constructed. This model will be utilised in formulating the system equations.

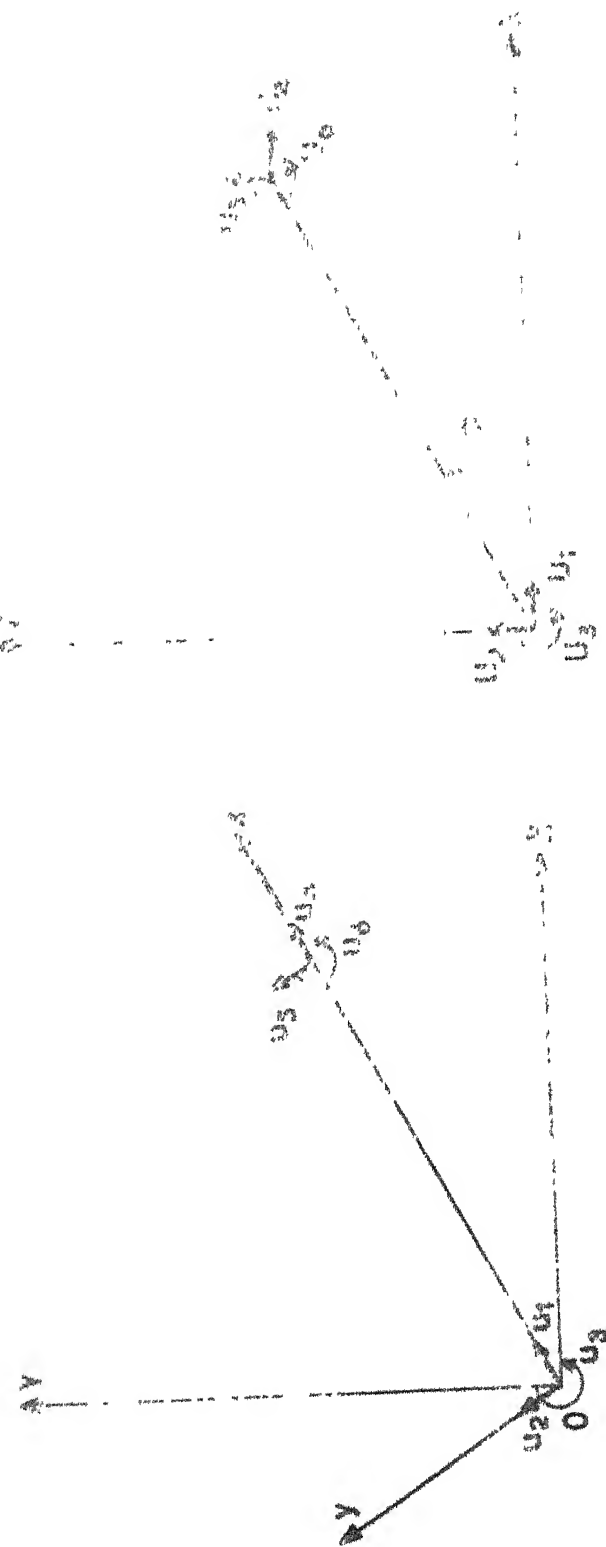
2.3 ELASTODYNAMIC MODELLING OF THE LINKAGE :

Elastodynamic analysis is the examination of displacement, velocity, stresses etc. of a moving elastic mechanism and inertia forces are calculated by assuming all the members rigid. Finite element method is utilised to perform the analysis. Modelling of the entire mechanism

that is conceiving the mechanism as collection of elements is essential as a first step. It is mentioned here (again) that the input crank is modeled as cantilever beam which eliminates the need for removing rigid body degrees of freedom. Elastodynamic analysis of a mechanism in motion helps in gaining insight into the elastic behaviour of different members under the dynamic conditions.

2.3.1 ELEMENT MATRICES:

In order to construct the finite element model each member of the linkage is taken as an element. Usually a link is modeled as a planar beam element used in structure. For a generalized planar element 6 degrees of freedom, 3 at each end (node) is sufficient to completely describe elastic deformation of the element. This is shown in (Fig. 2.6) in a 2-D frame. u_1 and u_4 are axial elastic deformation coordinates. u_2, u_3 and u_5, u_6 account for the transverse deflection characteristic of the element. u_1 to u_6 forms a generalised set of coordinates. They are defined as function of co-ordinates and time in the case of deriving element matrices for a link. The co-ordinates defining the axial deflections, a linear interpolation model (mode shape) is used. That is linear function of the co-ordinate defined along the element length. For the transverse displacements



ELEMENT IN GLOBAL CO-ORDINATE SYSTEM
ELEMENT CO-ORDINATE SYSTEM (X Y)
 u_1, u_2, u_3

A GENERAL PLANAR BEAM ELEMENT IN
ELEMENT-ORIENTED CO-ORDINATE FRAME (X Y)
 u_1, u_2, u_3

FIG. 2.6

a cubic interpolation function is assumed. Using linear superposition theory the two deflection patterns are superimposed so that complete elastic behaviour of the element is described. From equilibrium equations the element mass and stiffness matrices are derived [8]. They are same with the stiffness and mass matrices of a planar frame element with 6 d.o.f.

The generalised form of these matrices are given below. It is noted that these are element oriented element matrices and independent of system configuration.

The element stiffness matrix $[k]$ is

$$[k] = \begin{bmatrix} EA/L & & & & & \\ 0 & 12EI/L^3 & & & & \\ 0 & 6EI/L^2 & 4EI/L & & & \text{Symmetric} \\ -EA/L & 0 & 0 & EA/L & & \\ 0 & -12EI/L^3 & -6EI/L^2 & 0 & 12EI/L^3 & \\ 0 & 6EI/L^2 & 2EI/L & 0 & -6EI/L^2 & 4EI/L \\ & & & & & \dots (2.13) \end{bmatrix}$$

The element mass matrix $[m]$ is

$$\begin{bmatrix}
 1/3 & & & & \\
 0 & 13/35 & & & \text{Symmetric} \\
 0 & 11L/210 & L^2/105 & & \\
 \hline
 [m] & 1/6 & 0 & 0 & 1/3 \\
 0 & 9/70 & 13L/420 & 0 & 13/35 \\
 0 & -13L/420 & -L^2/140 & 0 & -11L/210 & L^2/105 \\
 \hline
 & & & & & \gamma_{AL} \\
 & & & & & \dots\dots (2.14)
 \end{bmatrix}$$

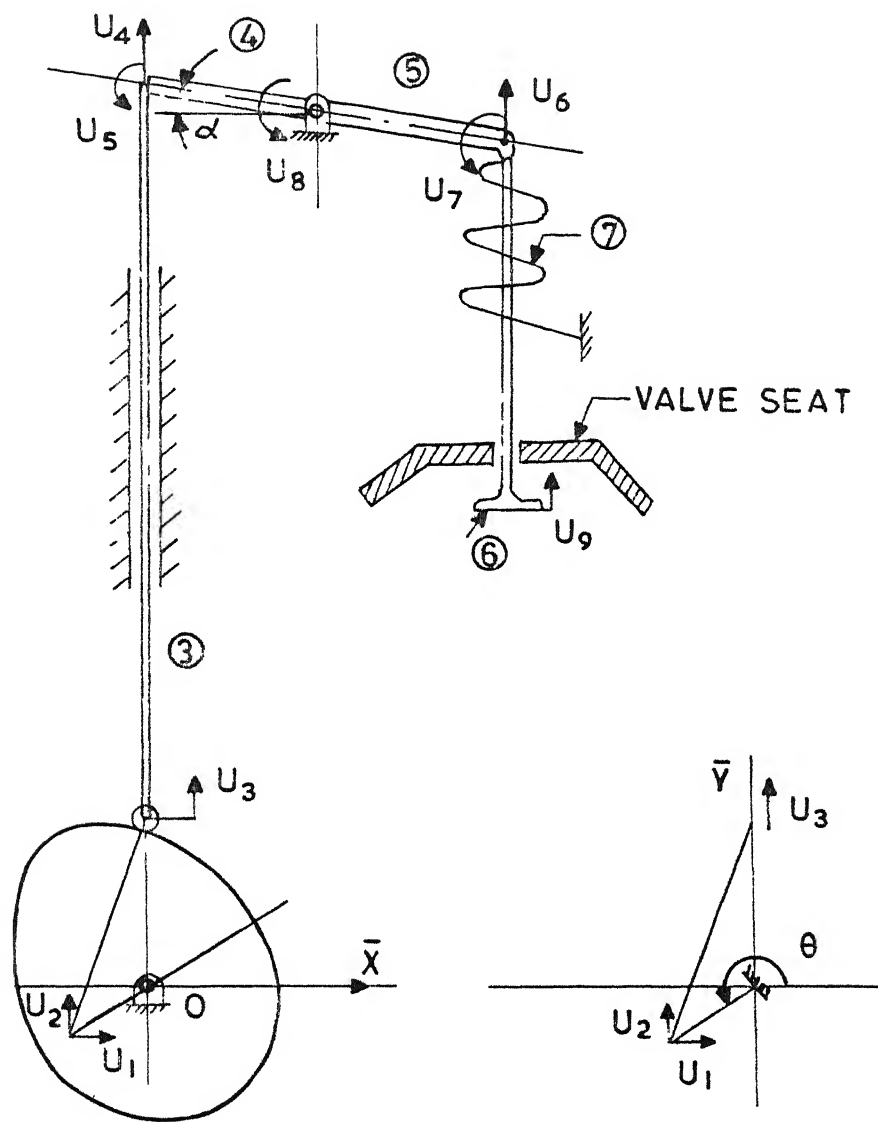
E is the young's modulus of the material of the element, A is the uniform cross-sectional area of the link, L is length of the link and I is moment of inertia of the cross-sectional area, γ_{AL} mass of the element. The effect of rotary inertia and shear are not included in the derivation of element matrices. The mass matrix given here is a consistent mass matrix.

2.3.2 SYSTEM MODEL :

Section 2.2 describes an approach to represent the cam-follower pair into its equivalent lower pair system which can show the same dynamic and elastic behaviour as that of the actual system. Once this is accomplished the rest of the follower train along with this model can be represented by forming a system model to perform the deflection analysis.

To construct the model of the entire system, system co-ordinates are to be defined at element node. (Fig 2.8) shows the system co-ordinates of the complete valve-train model. The system is consisted of total 7 elements and they are the numbers in the circles. It is noted that the system configuration that is shown in (Fig. 2.8) is for a particular geometric configuration of the cam profile which is taken care by the equivalent links. The system reference frame is $\bar{X}-\bar{Y}$. The crank inclines at an angle of Θ w.r.t. the \bar{X} .

The follower train has 5 elements. All are modeled as a planer frame element. The stiffness of return spring has its own spring index. Usually, the rocker arm has got peculiar shape. It is considered to be of two elements. One for the left rocker arm and the other for the right rocker arm. For modelling purposes they are approximated as beams with uniform rectangular cross-section. One can take more accurate model of the rocker arm by constructing a 2-dimensional or 3- dimensional finite element mesh. After formulating a more precise model the no. of degree of freedom could be reduced [19] so as to match element co-ordinates. Thus the basic analysis approach remains same but one pays heavy computational cost to obtain finer precision of the final answer.



INPUT CRANK MODELED
AS CANTILEVER BEAM.

IDEALIZED MODEL OF THE SYSTEM U_1 --- U_9
SHOWS THE SYSTEM CO-ORDINATES.

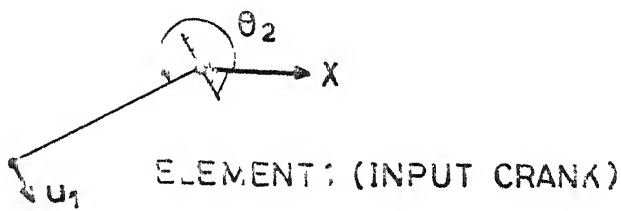
FIG. 2.8

The angle α (see Fig. 2.8) is a very small inclination of the rocker arm. In automotive cams the total follower rigid body displacement is not high compared to the dimension of the links of the follower train. The angle α actually takes care of the variation (small) in geometry. During rise or return period of the cam the rocker arm's geometric configuration is specified by this angle α . Value of α can be obtained by dividing the rigid body displacement at that instant with the lower rocker arm length.

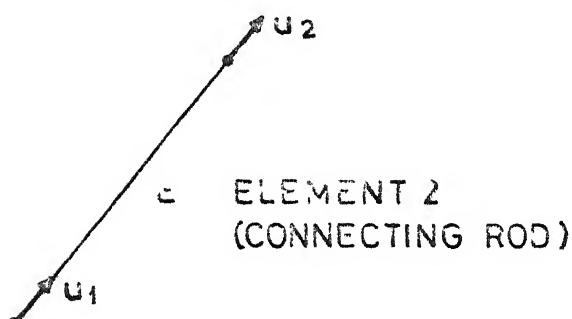
Total of 9 system co-ordinates U is defined for the system model. To formulate the system equation of motions the element property matrices are to be generated in terms of system co-ordinates, so that the total system matrices are formed.

Fig.2.7 shows a generalised element in system oriented element co-ordinates. In case of a mechanism the different links take various geometric orientation throughout the course of the motion of input link. Thus element matrices are needed to be written down in system-coordinate form. The transformation from the element oriented element coordinates to system oriented element co-ordinates is accomplished by a transformation matrix $[R]$. The general form of

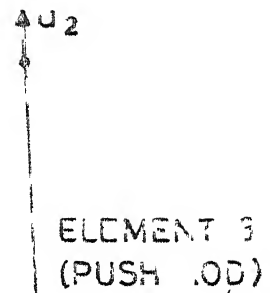
$$[R] \text{ is } \begin{bmatrix} A & 0 \\ 0 & A \end{bmatrix} \quad \dots (2.15)$$



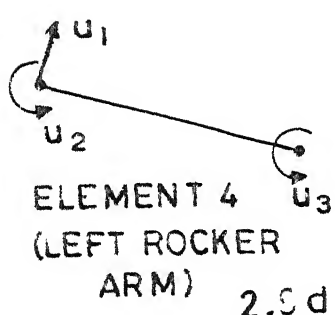
2.9a



2.9b



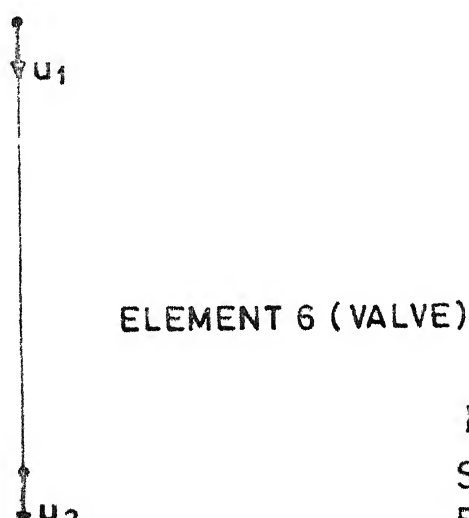
2.9c



2.9d



2.9e



2.9f

FIG. 2.9a ----- 2.9f
SHOWING THE INDIVIDUAL
ELEMENT CO-ORDINATES.

where A is given as

$$\begin{bmatrix} \cos\phi & \sin\phi & 0 \\ -\sin\phi & \cos\phi & 0 \\ 0 & 0 & 1 \end{bmatrix}$$

where ϕ is as given in Fig. 2.7.

The element mass and stiffness matrices for all the 7 elements are given in expressions (2.15a) to (2.15g). These are obtained for the corresponding element co-ordinates. The element co-ordinates are shown in (Fig 2.9a to 2.9f) for each element. Transforming them to system oriented element co-ordinates the transformation matrices are necessary. These transformation matrices $[B]$ take into account the change in geometry. The six transformation matrices are given in equations (2.15h - 2.15m).

The element coordinates and system coordinates are related by

$$\{u\} = [B] \{U\} \quad \dots (2.16)$$

for each element.

The system oriented element mass and stiffness matrices are expressed as

$$[\bar{k}]_i = [B]_i^T [k]_i [B]_i \quad \dots (2.17)$$

$$[\bar{m}]_i = [B]_i^T [m]_i [B]_i \quad \dots (2.18)$$

i varies from 1 to no. of elements.

Element 1

$[m] = E\eta I$, to be calculated from (2.7) in
section 2.2. (2.15a)

$[k]$, to be calculated from appendix II.

Element 2

$[k] = K_H \begin{bmatrix} 1 & -1 \\ -1 & 1 \end{bmatrix}$, here the coefficient are
used considering longitudinal
deflections. (2.15b)

Element 3

$[k] = \frac{E_3 A_3}{L_3} \begin{bmatrix} 1 & -1 \\ -1 & 1 \end{bmatrix}$ (2.15c)

$[m] = \gamma A_3 L_3 \begin{bmatrix} 1/3 & 1/6 \\ 1/6 & 1/3 \end{bmatrix}$

Element 4

$[k] = \begin{bmatrix} \frac{12E_4 I_4}{L_4^3} & & \\ & \frac{6E_4 I_4}{L_4^2} & \frac{4E_4 I_4}{L_4} \\ & \frac{6E_4 I_4}{L_4^2} & \frac{2E_4 I_4}{L_4} & \frac{4E_4 L_4}{L_4} \end{bmatrix}$ Symmetric (2.15d)

$$[m] = \gamma A_4 L_4$$

$$\begin{bmatrix} \frac{13}{35} & & & \\ \frac{11L_4}{210} & \frac{L_4^2}{105} & & \\ -\frac{13L_4}{420} & -\frac{L_4^2}{140} & \frac{L_4^2}{105} & \\ \end{bmatrix} \quad \text{Symmetric}$$

Element 5

$$[m] = \gamma A_5 L_5$$

$$\begin{bmatrix} \frac{L_5^2}{105} & & & \\ \frac{13L_5}{420} & \frac{13}{35} & & \\ -\frac{L_5^2}{140} & \frac{11L_5}{210} & \frac{2}{105} & \\ \end{bmatrix} \quad \text{Symmetric}$$

..... (2.15e)

$$[k] =$$

$$\begin{bmatrix} \frac{4E_5 I_5}{L_5} & & & \\ \frac{6E_5 I_5}{L_5^2} & \frac{12E_5 L_5}{L_5^3} & & \\ \frac{2E_5 I_5}{L_5} & \frac{-6E_5 I_5}{L_5^2} & \frac{4E_5 I_5}{L_5} & \\ \end{bmatrix} \quad \text{Symmetric}$$

Element 6

$$[m] = \gamma A_6 L_6 \begin{bmatrix} 1/3 & 1/6 \\ 1/6 & 1/3 \end{bmatrix} \dots (2.15f)$$

$$[k] = \frac{E_6 A_6}{L_6} \begin{bmatrix} 1 & 1 \\ -1 & 1 \end{bmatrix}$$

Element 7

$$[m] = \text{mass of return spring} \dots (2.15g)$$

$$[k] = \text{spring stiffness}$$

since only one element co-ordinate is assigned to the spring.

The transformations matrices are as follows:

$$[B]_1 = \{ \sin\theta_1 \ - \cos\theta_1 \} \dots (2.15h)$$

$$[B]_2 = \begin{bmatrix} \cos\theta_2 & \sin\theta_2 & 0 \\ 0 & 0 & \sin\theta_2 \end{bmatrix} \dots (2.15i)$$

$$[B]_3 = \begin{bmatrix} 1 & 0 \\ 0 & 1 \end{bmatrix} \dots (2.15j)$$

$$[B]_4 = \begin{bmatrix} \cos\theta_3 & 0 & 0 \\ 0 & 1 & 0 \\ 0 & 0 & 1 \end{bmatrix} \dots (2.15k)$$

$$[B]_5 = \begin{bmatrix} 1 & 0 & 0 \\ 0 & \cos\theta_3 & 0 \\ 0 & 0 & 1 \end{bmatrix} \dots (2.15l)$$

$$[B]_6 = \begin{bmatrix} -1 & 0 \\ 0 & -1 \end{bmatrix} \dots (2.15m)$$

It is to be noted that $[\bar{k}]_i$ and $[\bar{m}]_i$ are function of input geometric parameter i.e. crank angle θ . Thus at every instant $[\bar{k}]$ and $[\bar{m}]$ are expected to vary.

Having obtained the element matrices in the global frame the next job is systematic assembly of all the element matrices so as to get total system mass and stiffness matrices.

The system mass matrix $[M]$ and system stiffness matrix $[K]$ are given by the following expressions

$$[M] = \sum_{i=1}^{NE} [\bar{m}]_i \quad \dots \dots (2.19)$$

$$[K] = \sum_{i=1}^{NE} [\bar{k}]_i \quad \dots \dots (2.20)$$

Where NE = no. of elements. The order of these matrices are equal to no. of system co-ordinate. Several computational schemes are available in order to assemble the element matrices. e.g., permutation vector method, code system of assembly [13] etc. Here code-system is selected for assembly, because the flexibility in numbering the system coordinates features it's advantage.

Finally, with this matrices determined the dynamic equation of motion for the system under study is represented in the form as follows.

$$[M]\{\ddot{U}\} + [C]\{\dot{U}\} + [K]\{U\} = \{F\} \quad \dots \dots (2.21)$$

The equation (2.21) is written in terms unknown global co-ordinates. It is actually a set of differential equations. The $[C]$ matrix is system damping matrix, about which discussion is there in section 2.4.2. Vector $\{F\}$ contains the inertia forces due to the gross motion (Rigid-body) of the mechanism plus any additional external forces if present. Equation (2.21) is the mathematical representation of the system model.

2.4 ANALYSIS APPROACH :

2.4.1 METHODOLOGY :

The finite element displacement method is used efficiently in the elasto-dynamic analysis. A mechanism unlike a structure changes its position w.r.t. the fixed frame when it rotates. Thus the continuous rotation of the mechanism is divided into small time intervals. The continuous rotation can be more accurately taken care of in modelling if a coordinate is defined corresponding to the rigid body degree of freedom of the mechanism. In the present work no such coordinate is defined at the rotation end and thus elimination of rigid body degrees of freedom to make the system stiffness matrix non-singular is avoided. During

each interval the linkage takes a certain geometric orientation according to its motion characteristics. At each such linkage configuration the mechanism is converted into a structure by diminishing its rigid body degree of freedom. The modelling of input crank as a cantilever is used to do this.

At each such configuration the mass, stiffness properties of the mechanism treated as an elastic structural system are derived and assumed to remain unchanged during the interval. At this position the forces acting on this 'structure' are the rigid body inertia forces due to gross rigid body accelerations of the elements plus any external forces. The deflections are calculated solving the set of equations of motion. The next mechanism configuration is considered and the same procedure is followed.

Elasto-dynamic analysis of a linkage using finite element approach essentially involves the following sequence of steps:

(i) the idealization of the linkage structure is needed; this will require the selection of the type and size of the finite element to generate the system mesh.

(ii) the system oriented mass and stiffness matrices are generated for each element.

(iii) the element mass and stiffness matrices are superposed/ assembled systematically to develop mass and stiffness of the total structure of the system of linkage.

(iv) determination of the unknown nodal displacements is made by solving a system of coupled ordinary differential equations.

(v) all required numbers such as stress strains associated with the problem are computed.

Previous section of this chapter (2.3.1, 2.3.2) discuss about the implementation of first 3 steps given above. The solution procedure is discussed in the next section.

2.4.2. SOLUTION PROCEDURE :

The equation of motion developed in section 2.3.2 is rewritten here.

$$[M]\{\ddot{U}\} + [C]\{\dot{U}\} + [K]\{U\} = \{F\} \quad \dots (2.22)$$

This represent a set of coupled ordinary differential equations. The involving terms are already explained in previous sections. Damping effect is incorporated

in the form of system damping matrix $[C]$. The complete solution of the equation (2.22) consists of accomplishing 3 parts.

(i) determination of eigenvalues and eigenvectors of the corresponding homogeneous equation.

$$[M]\{\ddot{U}\} + [K]\{U\} = 0 \quad \dots \dots (2.23)$$

The effect of damping on the eigenvalues and eigenvectors is assumed to be negligible.

(ii) transformation of this set of coupled equations into a set of uncoupled equations expressed in the form of normal co-ordinates.

(iii) solve for the complete solution of the vector U .

The implementation of the first step that is the determination of eigensystem is described in Appendix III.

To transform the set of coupled equations into a set of uncoupled equations the system co-ordinates U are converted to normal coordinates as shown below

$$\{U\} = [\phi]\{\eta\} \quad \dots \dots (2.24)$$

where $\{\eta(t)\}$ is the displacement vector in normal coordinate.

$[\phi]$ represents the modal matrix which contains resulting eigenvectors columnwise as calculated in step (i). $[\phi]$ remain constant during the chosen interval.

Successive differentiation of equation (2.24) yields the following two equations

$$U = [\phi] \{ \ddot{\eta} \} \quad \dots \dots (2.25)$$

$$\text{and} \quad \ddot{U} = [\phi] \{ \ddot{\eta} \} \quad \dots \dots (2.26)$$

substituting equations (2.24), (2.25), and (2.26) in equation (2.22) it can be rewritten as

$$[M] [\phi] \{ \ddot{\eta} \} + [C] [\phi] \{ \dot{\eta} \} + [K] [\phi] \{ \eta \} = \{ F \} \dots \dots (2.27)$$

Premultiplying this equation by $[\phi]^T$ and using the orthogonality properties the equation formed is as in (2.28).

$$[\bar{M}] \{ \ddot{\eta} \} + [\bar{C}] \{ \dot{\eta} \} + [\bar{K}] \{ \eta \} = [\phi]^T \{ F \} \quad \dots \dots (2.28)$$

where,

$$\begin{aligned} [\bar{M}] &= [\phi]^T [M] [\phi] \\ [\bar{K}] &= [\phi]^T [K] [\phi] \\ [\bar{C}] &= [\phi]^T [C] [\phi] \end{aligned} \quad \dots \dots (2.29)$$

All the matrices $[\bar{M}], [\bar{K}], [\bar{C}]$ are diagonal matrices. Generally, the system damping matrix $[C]$ is taken as proportional to either $[M]$ or $[K]$ or a linear combination of them. Obviously, the matrix $[\bar{C}]$ will also be diagonal. But the use of a single constant to represent the damping characteristics of the systems with multiple degrees of freedom is not realistic. For this reason, the standard practice is to consider $[\bar{C}]$ as

proportional to the critical damping of the system at the normal mode [9]. Again the matrix $[\tilde{C}]$ becomes diagonal and equation (2.22) becomes uncoupled. These uncoupled equation assume the following form,

$$\tilde{m}_i \ddot{\eta}_i(t) + 2\omega_i \xi_i \tilde{m}_i \dot{\eta}_i(t) + \tilde{k}_i \eta_i(t) = p_i \dots (2.30)$$

$i = 1, 2, \dots, m$, ; m = no. of modes found out in eigen system.

The above equation represents the i -th equation of the set of resulting uncoupled differential equations. The associated terms are

- η_i = displacement at the i -th normal coordinate
- $\dot{\eta}_i$ = velocity at the i -th normal coordinate
- $\ddot{\eta}_i$ = accelerations at the i -th normal coordinate
- \tilde{m}_i = i -th diagonal of $[\tilde{M}]$
- \tilde{k}_i = i -th diagonal of $[\tilde{K}]$
- p_i = i -th element of $[\phi]^T \{F\}$
- ω_i = i -th natural frequency
- $2m_i \omega_i$ = critical damping at the i -th normal mode
- ξ_i = damping ratio (actual damping / critical damping) at the i th normal mode .

Matrix $[\bar{C}]$ for the choice of damping in (2.30) is

$$[\bar{C}] = 2 \begin{bmatrix} \omega_1 \zeta_1 & & \\ & \omega_2 \zeta_2 & \\ & & \omega_m \zeta_m \end{bmatrix} \quad [\bar{M}] \dots (2.31)$$

As the damping is chosen to be proportional to the critical damping the matrices $[C]$ and $[\bar{C}]$ are never required in actual computation.

$$\text{Noting that } [\bar{K}] = [\omega^2] [\bar{M}] \dots (2.32)$$

where $[\omega^2]$ is also a diagonal matrix, equation (2.30) can be rewritten as

$$\ddot{\eta}_i(t) + 2\omega_1 \zeta_i \dot{\eta}_i(t) + \omega_1^2 \eta_i(t) = \bar{p}_i \dots (2.33)$$

$$\text{where, } \bar{p}_i = \frac{p_i}{m_i} \dots (2.34)$$

Each element of p_i is assumed to remain constant during the current interval.

The solution of the equation (2.33) is given as [17]

$$\eta_i(t) = \frac{\bar{p}_i}{\omega_1^2} + e^{-\zeta_1 \omega_1 t} \left[A_1 \cos(\mu_i t) + \frac{B_1}{\sqrt{1-\zeta_1^2}} \sin(\mu_i t) \right] \dots (2.35)$$

Where first term is the particular Integral, and second term is the homogeneous solution.

$$\text{where, } \dot{\eta}_1 = \sqrt{\frac{\omega_1^2}{1 - \frac{\omega_1^2}{\omega_i^2}}} \omega_i \quad \dots \quad (2.36)$$

$$\dot{\eta}_1 = \eta_1(0) - \frac{\dot{\eta}_1}{\omega_1^2} \quad \dots \quad (2.37)$$

$$\dot{\eta}_1 = \frac{\eta_1(0)}{\omega_1} + \frac{c}{\omega_1} \omega_1 A_1 \quad \dots \quad (2.38)$$

$\eta_1(0)$ and $\dot{\eta}_1(0)$ are the i th initial value of the displacement and velocity of the vector η .

The displacement η determined from equation (2.35) are transformed back to system coordinate U with the aid of the equation (2.24). Finally the unknown nodal displacements are calculated out. If one wishes he can also find out the system oriented element co-ordinates employing the matrix used for assembly of all element matrices.

2.4.3 FORCE VECTOR :

The force vector $\{F\}$ in equation (2.22) consists of inertia forces due to rigid body motion. $\{F\}$ is obtained by multiplying the system mass matrix with negative of acceleration vector .

$$\{F\} = - [M] \{R\} \quad \dots \quad (2.39)$$

where , R = rigid body acceleration vector along the system coordinate. In this approach variation of acceleration

over the link lengths is not considered. $\{F\}$ during each interval is assumed to remain constant.

It can be said from section 2.1 that the acceleration of the roller centre (see Fig. 2.1) and that of the slider are same instantaneously. The slider acceleration can be computed from the expression (2.40)[16].

$$a_s = - \omega_2^2 r_1 [\sin \theta_2 + \frac{n^2 \cos(180-2\theta_2) + \cos^4 \theta_2}{(n^2 - \cos^2 \theta_2)^{3/2}}] \quad \dots \dots (2.40)$$

where, ω_2 = constant angular velocity of the crank

$$n = \frac{r_2}{r_1}$$

a_s = slider acceleration .

Acceleration of the push rod is same as the roller centre. The valve-end of rocker arm moves with an acceleration.

$$a_v = - C \times a_s \quad \dots \dots (2.41)$$

where, C is the lever ratio of rocker arm, '-' sign indicates the opposite direction.

At this iteration the return spring force is also active which is the product of spring stiffness and spring deflection (rigid). This force is added with corresponding element in the vector $\{F\}$ and the resulting $\{F\}$ is obtained.

CHAPTER III

COMPUTER PROGRAMS

For the purpose of implementing the steps presented in the section (2.4.1) analysis approach a computer program has been developed. The aim is to find out the solution of the equations (2.22) which in turn produces the displacement vector $\{U\}$. The program is written in FORTRAN-IV and run on DEC-1090 system.

BASIC COMPUTATIONAL STEPS:

(i) Read all the data describing the geometry of the follower linkage (i.e. link dimensions), material property , return spring stiffness etc. The data related to element assembly are also read in input.

(ii) Get the data for individual masses and lengths of the equivalent links of the cam-follower through a separate subroutine.

(iii) Compute the stiffness and mass properties of each element employing equations (2.15 a - 2.15 g).

(iv) Starting from an initial position of the cam (the initial position of the crank is derived from

this is to transform the element matrices in step (iii) to the system oriented co-ordinate system.

(v) Assemble all the system oriented element matrices to form a total system mass and stiffness matrices $[M]$ and $[K]$ respectively.

(vi) Solve the eigen value problem as described in equation (2.23) to find all the eigen-values and find the modal matrix $[\phi]$ consisting of eigen vectors.

(vii) Compute the force vector (section 2.4.3) in global co-ordinate frame.

(viii) Uncouple the system governing equations (2.22) and solve for the displacement vector η in normal co-ordinates.

(ix) Transform the vector $\{\eta\}$ to obtain $\{U\}$ by the expression (2.24).

(x) Go to the next cam position by adding the incremental angle with the current angle and repeat the entire steps from step (ii) to step (x) except step (iii) until the final cam position is reached.

87513

SUBROUTINES :

Following subroutines are used to back the main program.

- (1) ELMCON : This subroutine forms the element mass and stiffness matrices in element oriented co-ordinate system and then convert them to system oriented frame. This routine is invoked by the routine SYSMAT.
- (2) TRANS : This routine is used to calculate the transformation matrix corresponding to each element for successive cam position or crank position. The routine ELMCON calls this routine, for transformation.
- (3) SYSMAT: This subroutine serves the purpose of systematic assembly of all element matrices provided by routine ELMCON.
- (4) JACOBI: This routine solves the generalised eigenvalue problem. $AX = \lambda BX$. It makes use of the generalised Jacobin algorithm. The output of this routine is modal matrix $[\phi]$ of the order NSC \times NSC where NSC is total no. of system co-ordinate and eigen vector λ of order NSC.

(5) SOLVE : The solution of the system's dynamic equation of motions (2.22) is done by this routine. It invokes the routine JACOBI and check for the orthogonalities properties i.e., $[\phi]^T [K] [\phi] = [\lambda]$ and $[\phi]^T [M] [\phi] = [I]$, $[I]$ is an identity matrix , The vectors η and final displacement vector U are then determined by this routine.

(6) EQLINI: The equivalent link lengths and their included angle with reference to fixed frame are produced by this routine. The rigid body displacement at the cam end is also output of this routine.

(7) FORSV: This subroutine is used to calculate force vector representing the R.H.S of the equation of motion (2.22).
Apart from the above routines function subprograms are used to determine stiffness of the crank, connecting rod in the equivalent mechanism and mass of the crank.

CHAPTER IV
COMPUTATIONAL WORK

To judge the workability of the analytical treatments presented in Chapter II a numerical example is solved by means of a computer program (Chapter III). Computational observation and discussions are depicted in this chapter.

4.1 NUMERICAL EXAMPLE:

The numerical example that is taken up contains a cam of the type DRRD (i.e., Dwell-Rise-Return-Dwell) which is very common in automotive overhead valve train linkage. The cam is shown in (Fig. 4.1). It is comprised of 3 circular arcs for the rise-return portion. Other input data pertaining to the rest of the mechanism that is of the follower train are given below :

Length of the Pushrod	- 22.0 cm.
Diameter of the Pushrod	- 1.5 cm.
Length of the left rocker arm	- 4.5 cm.
Cross Sectional area	- $(2.0 \times 1.0) \text{ cm}^2$
Length of the right rocker arm	- 5.5 cm.
Cross -section area	- $(2.0 \times 1.0) \text{ cm}^2$.
Length of the valve	- 9.0 cm
Dia. of the valve	- 1.5 cm

$r_o = 1.0 \text{ cm}$
 $R_1 = R_3 = 7.0 \text{ cm}$
 $R_2 = 3.0 \text{ cm}$
 $R_b = \text{ROLLER RAD'US} = 0.8 \text{ cm}$

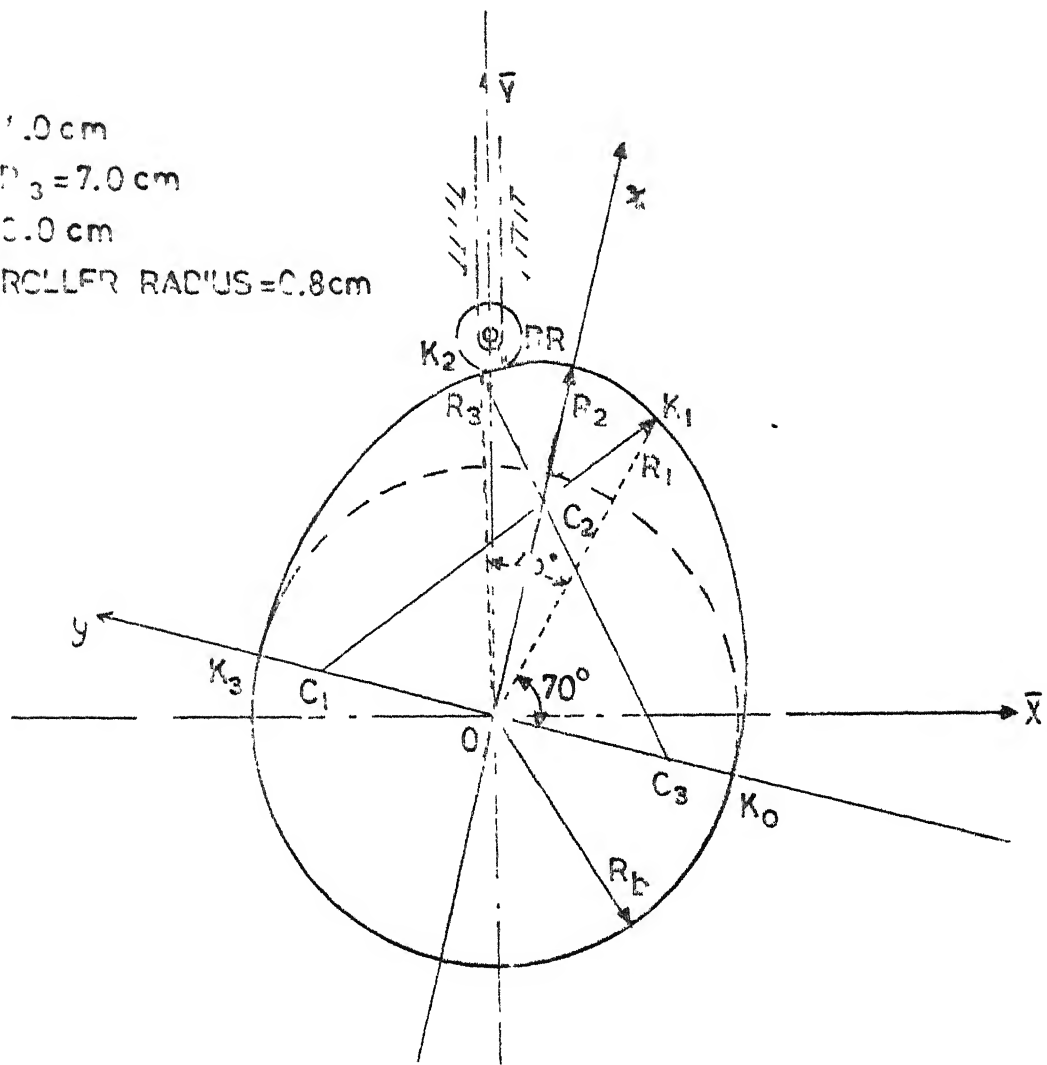


FIG. 4.1 CAM PROFILE FOR THE NUMERICAL EXAMPLE.

Return spring stiffness	- 40.0 kgf/cm.
Roller radius	- 0.8 cm.
Young's Modulus of Steel	- 2.1×10^6 kgf/cm ² .
Poissons ratio	- 0.3
Material density	- 7.8×10^{-3} kg/cm ³
Damping ratio	is taken as - 0.05

The required data's for the cam profile and follower are shown in Fig. 4.1.

4.2 RESULTS AND DISCUSSIONS:

The cam profile that is being considered in this example shows 180 degrees of dwell characteristics. During the dwell period the follower does not execute any motion. Thus the analysis is performed within a range of 180 degree. The start of the rise (point K_0 in Fig. 4.1) is considered as initial position of cam (0 degree) and the end of return (point K_3) as final cam position (180 degree). C_1, C_2 etc. denotes the centre of curvature of respective profile region. But actually in one full rotation of cam the initial position is taken from dwell followed by rise, return and again dwell. For sake of analysis the cam rotation variation is illustrated from 0-180 degree in all figures. The analysis is carried out with an interval of 5 degree. The linkage is initialised for zero displacement velocity.

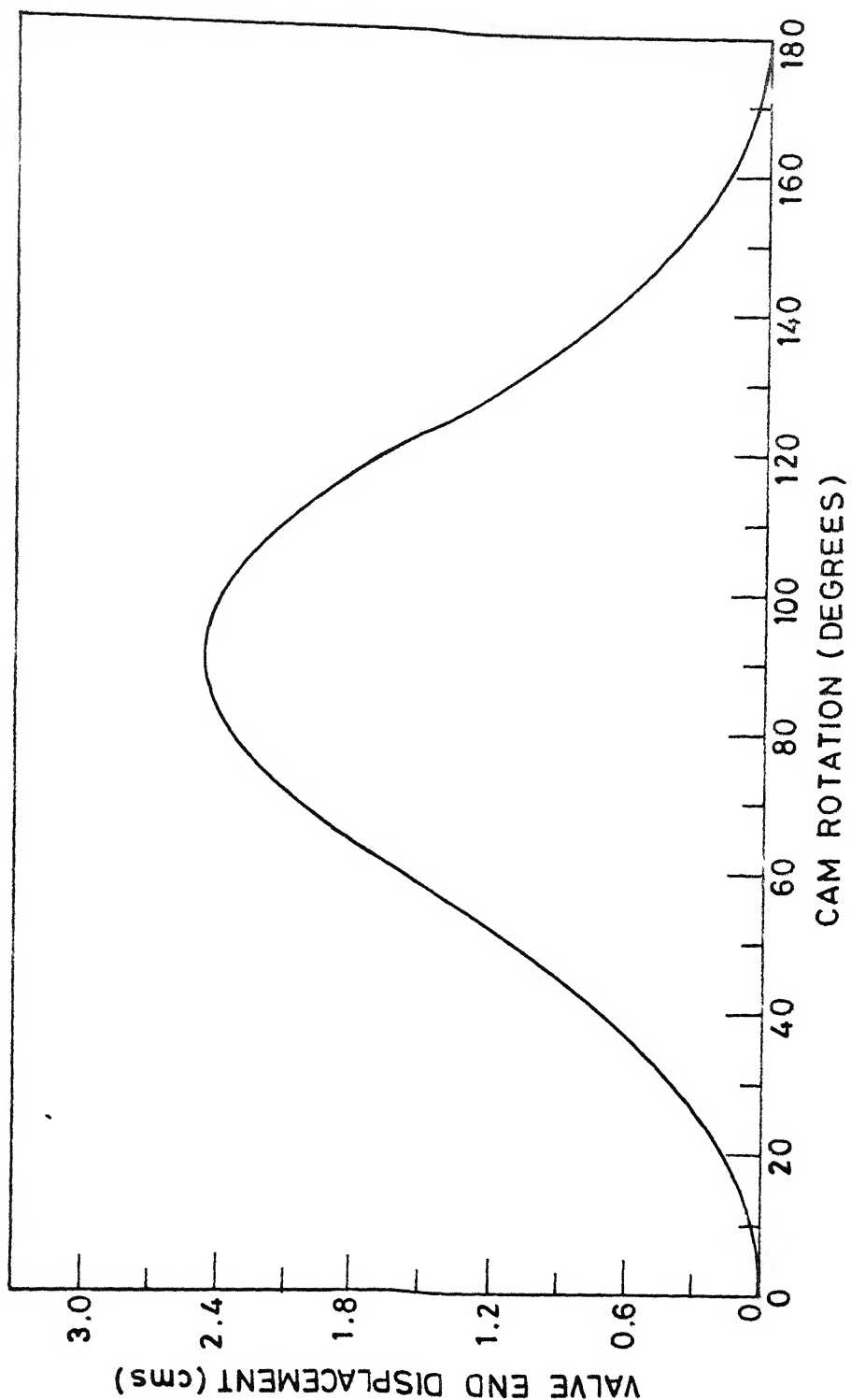


FIG. 4.2

The mass and stiffness values of the crank in the equivalent linkage for the present example are computed using the formula (2.7) and (2.9). These values are 0.5428 Kg and in the order of 10^8 kgf/cm respectively. The stiffness assigned to the connecting rod is found (eq. 2.12) out to be 0.3666×10^4 kg/cm. Though the connecting rod (link2) is assumed massless to avoid computational instability very small value of mass is considered for it.

The results of the deflection analysis are plotted for the node 9 (Fig. 2.8) that is at the valve end. Oftenly for automotive valve train cam linkage the displacement of the end mass is of paramount concern. Adherence to a prescribed motion characteristics of the end element i.e., of the valve determines the proper functioning of the entire unit. The error (or the difference between the cam command and follower response) may be represented by deflection at node 9 i.e., U_9 . Added with the rigid body displacement the net value may represent the total displacement of valve end.

The displacement characteristic of the cam profile is shown in (Fig. 4.2). The figure represents the rigid body displacement at the valve end for the rise-return portion. Fig. 4.3 shows the characteristics curves of

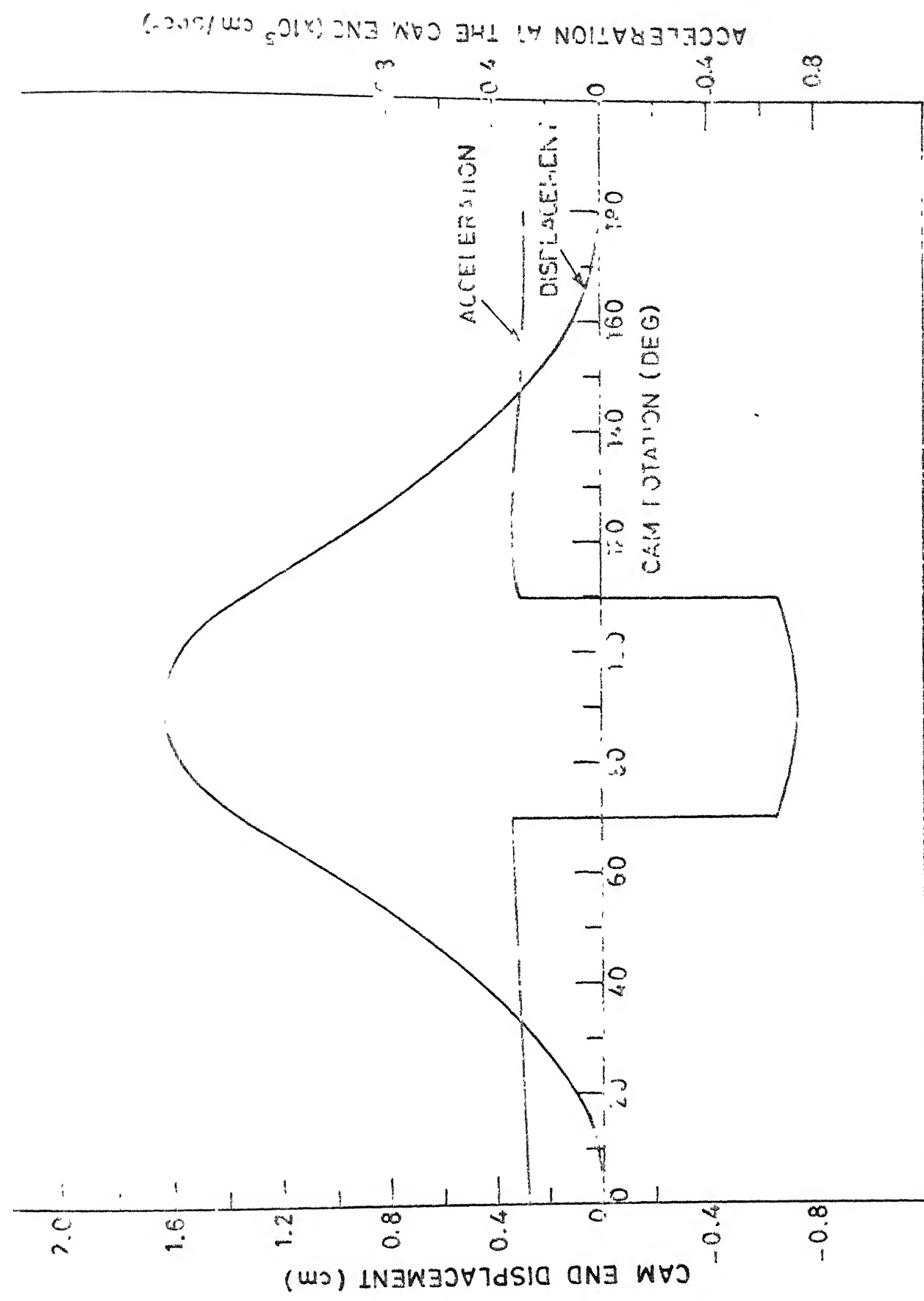


FIG. 4.3

the circular arc cam and translating roller follower for the example being considered. The displacement and acceleration are plotted against the cam rotation angle at the cam end. The curves are shown for both the rise return portion and the rise is started to be shown from 0 degree. But actually in the case of a DRRD cam this would be 90° and the end of return 270° . It is evident from the figure that the acceleration suddenly changes from positive value to negative value and the maximum negative acceleration is greater than the maximum positive one. This is observed at the blending point K_1 and at (K_2) , because at this particular point two equivalent slider-crank mechanism represent the cam motion. The symmetry is notable because of the symmetric shape of cam profile.

The elastic deflection at valve end (U_9) obtained by solving equation (2.21) and computed for each interval is shown in (Fig 4.4 and 4.5). This is plotted against the cam rotation and for various operating speed of the cam. At the starting of rise (0 deg.) the deflection is taken as zero. Few observations that are made are as follows:

(i) The shape and nature of the deflection curves resembles very much to that of acceleration curve (Fig. 4.2). This is expected because the forces (inertia force), that

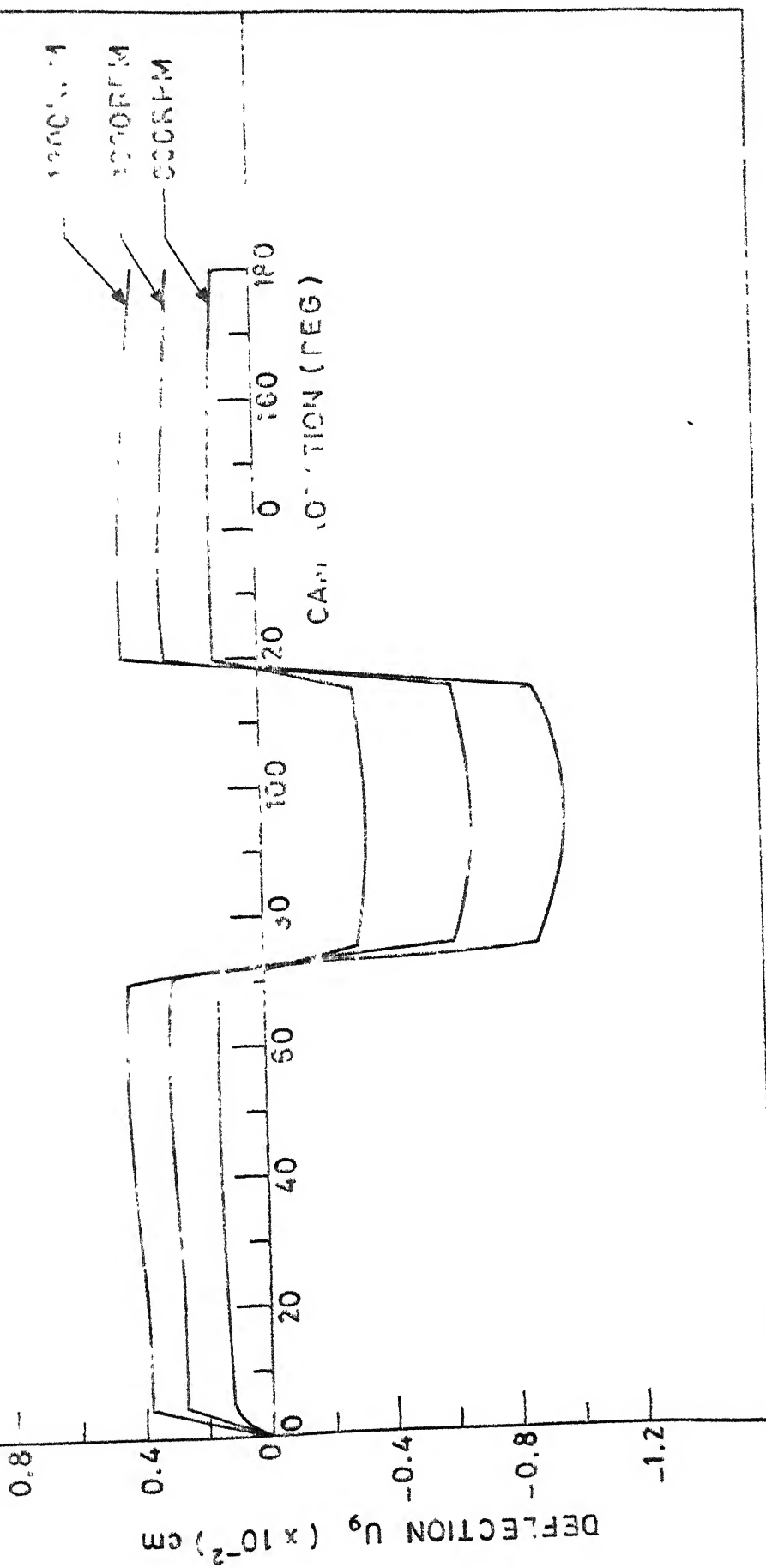
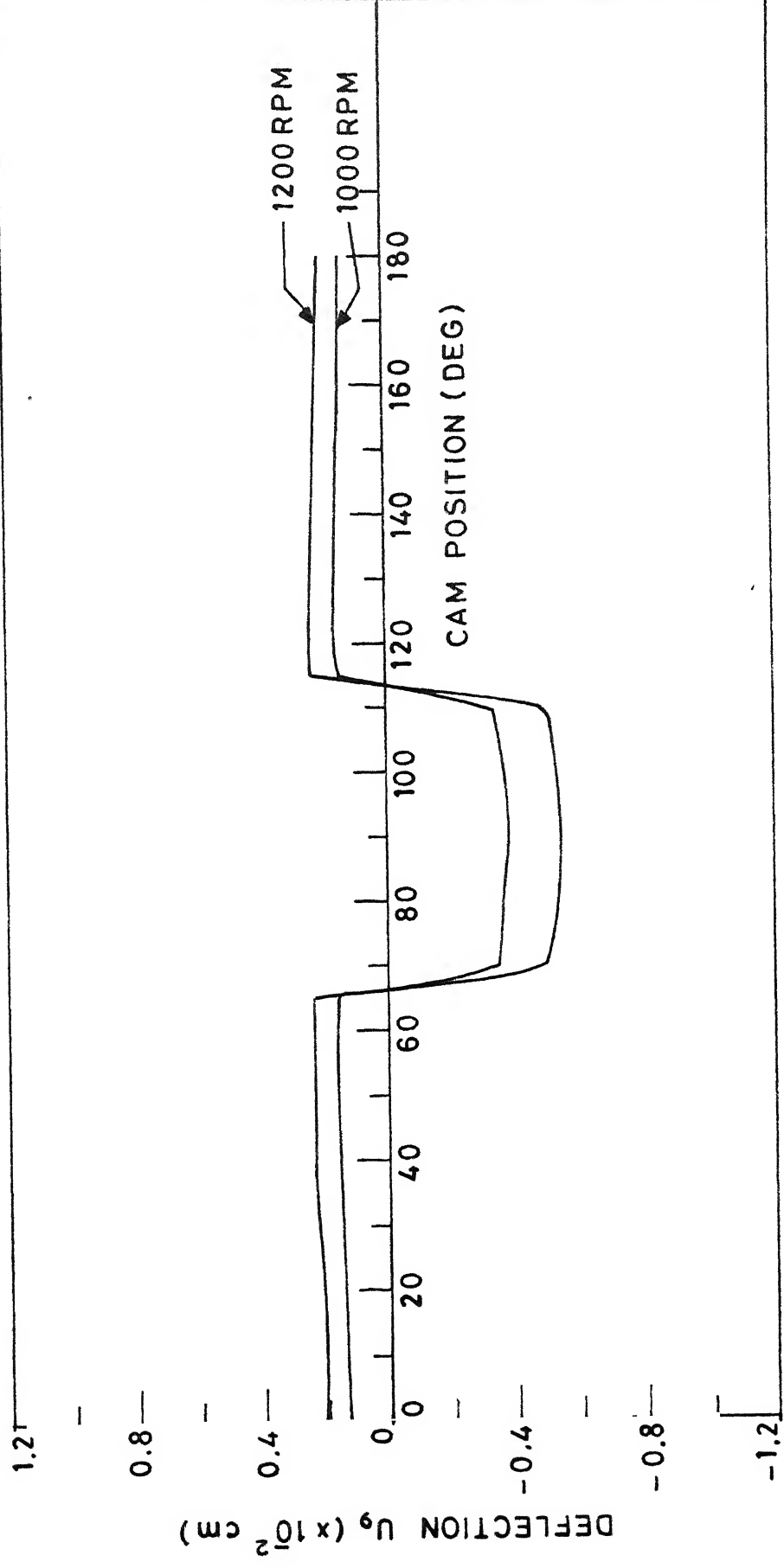


FIG. 4.4

cause deflections vary in the same manner as that of the acceleration curve against various successive geometric configuration.

(ii) The elastic deflection U_9 appears to remain almost constant on the portion K_0K_1 and K_2K_3 for various input speed. This deflection assumes higher value but in the opposite direction in nose portion (K_1K_2) of the cam compared to the other region of the profile. The marked differences of the deflection value on the two region may be attributed to the nature of acceleration and consequently the force in this region of cam profile. Equivalent link lengths are different that is the instantaneous 'structure' is also changed which changes the system stiffness and mass matrix. The difference between the maximum deflection and minimum deflection in the region K_1K_2 (Fig. 4.1) is much more pronounced at high speed (1800 rpm) compared to that at low speed (800 rpm). The curve shape is more flattened as the speed decreases. From the obtained result (not given) it is seen that deflection at low rpm (500) becomes too small and the total displacement curve at valve end almost coincides with the kinematic displacement curve.

Fig. 4.6 describes the deflection at node 9. These deflections are based on static analysis with the rigid body inertia forces as the force vector.. No Eigenvalue



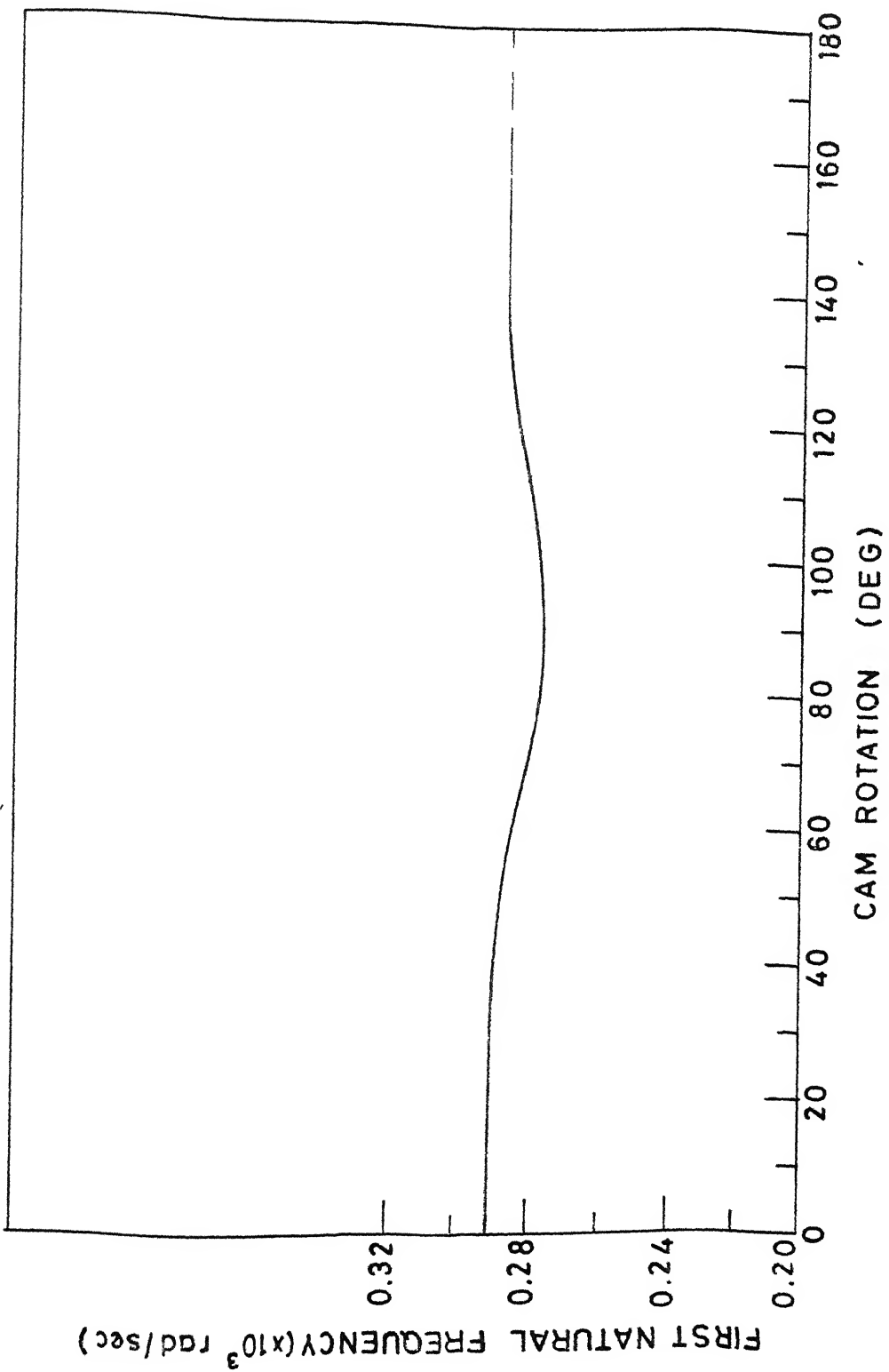


FIG. 4.7

problem is solved. These deflection are seen to be smaller than that solved through dynamic equation.

The natural frequencies of the linkage depend on its instantaneous configuration. The varying geometric configuration causes the natural frequency also to change. The nature of variation of first natural frequency with different cam position is illustrated in the (Fig. 4.7). The variation is seen to remain almost constant, in the flank portion, while variation is more prominent in nose region. This indicates that the change in configuration of the input crank affects insignificantly the system mass and stiffness properties in the region K_0K_1 and K_2K_3 .

CHAPTER V

CONCLUSIONS

5.1 TECHNICAL SUMMARY :

The technique of kinetoelastodynamic analysis of mechanism finds its importance in a situation where a mechanism is operated at high speed. The accuracy requirements in the output displacements, considerations of elasticity and dynamic factors in producing stress, strains deflection in high speed planar mechanisms are major problem which the rigidity assumption cannot overcome. KED, an advanced analysis and synthesis procedure is efficient in handling a circumstances which takes into accounts links flexibility, high inertia forces and provide means to obtain accurate solutions.

The applicability of the method was mainly limited to lower-pair planar mechanisms. Higher pair mechanism remain neglected in the context of using the method for better analysis. Cam mechanism, fall under higher pair classification and stand as an important part in the construction of modern day machinery. Evidences are plenty regarding the use of the mechanism. They are seen in automotive engines, aircraft engines, textile machines

and so on. A cam-actuated valve train linkage found in every automotive engine plays a responsible role in assisting to achieve the smooth operation of the engine. This, on the other hand, largely depends on the correct synthesis of the cam profile. The discrepancy existing between cam command and follower masses owing to the flexibility in the linkage needs correct evaluation for the betterment of the cam performance.

Conventional methods using lumped masses, spring etc. fail to provide a better analysis because of their certain inherent drawbacks. The necessity arises to exploit the potentiality of the newer methods so that a satisfactory and good analysis may be performed for cam activated valve train linkage. One faces difficulties while formulating an elastodynamic model of a cam mechanism because of the fact that the cam along with the follower does not match with the typical element shapes in elastodynamic literature in forming the cam as a known element. Certain considerations must be accounted so as to make the corresponding model of the cam follower possible and one can go ahead to model the entire linkage and perform the elastodynamic analysis. Thus some attempts may be tried in carrying out the analysis for the estimation of elastic deflections.

The objective in the present work is achieved in the following 2 phases :

(1) The equivalent model of the cam follower pair is proposed which shows kinematic equivalency and produces the approximately same elastic and dynamic behaviour as that of the actual system. The stiffness and masses of the links are derived from the above considerations and values are imparted to the equivalent links. These masses and stiffness do contribute towards the formation of total system mass and stiffness matrix.

(2) The elastic model of the entire system in terms of global co-ordinates is created. The equation of motion of the system is solved for the unknown nodal displacements. These displacements represent the elastic deflection at corresponding nodes.

The findings of the present work may be summarised as follows:

The elastic deflection at the valve end (error) increases with the increase in input speed. The nature of deflections depend on the cam profile characteristics. The natural frequency of the instantaneous structure does not vary largely with the variation of input crank position.

5.2 RECOMMENDATIONS:

In the beginning chapter the emphasis is placed on the fact that the present work is an attempt to analyse elastodynamically a cam-modulated linkage. In view of the limitations listed in section 1.5, the input crank is modeled as a cantilever beam. The modifications can be made by incorporating a coordinate at the support end of the crank thus taking care of the rigid body d.o.f. and the mechanism can be analysed under actual boundary conditions.

The equivalent model to replace the cam-follower pair can also be refined for more accurate representations of the dynamic and elastic behaviour of the actual cam-follower. Consequently the mass and stiffness assigned to crank and connecting rod will be more improved.

No distribution of the rigid body accelerations over the element length is assumed. Instead the inertia force (or body force) can be derived at the element level for each element and can be transformed to system reference frame to obtain the final force vector by assembling.

In this work each link is regarded as an element. For more accurate modelling particularly the pushrod and the valve can be subdivided into few elements inspite of one.

Appendix I

Determination of area moment of inertia of cam profile

A cam profile is shown in Fig. (A-1) which is pivoted at the point O. This profile is a convex profile. As mentioned in equation(2.3) the polar moment of inertia of the area (J_c ,area) is to be computed.

Consider a small sector bounded by r_i and r_{i+1} . The included angle is $\Delta\alpha$. The polar moment of inertia of this small sector may be given as $\frac{\Delta\alpha}{8} r_i^4$, about O

where $\bar{r}_i = \frac{r_i + r_{i+1}}{2}$ and sector is assumed as a small circular sector with mean radius \bar{r}_i . The total moment of inertia will be given [3] by

$$I = \sum_{i=1}^n \frac{\Delta\alpha}{8} \bar{r}_i^4$$

To calculate I the values r and θ are required for n no. of points on the profile. When a cam profile is known completely $r_i \theta_i$ can be computed for all i. For a cam with dwell, only in the rise-return portion the values of r, θ have to be calculated.

4

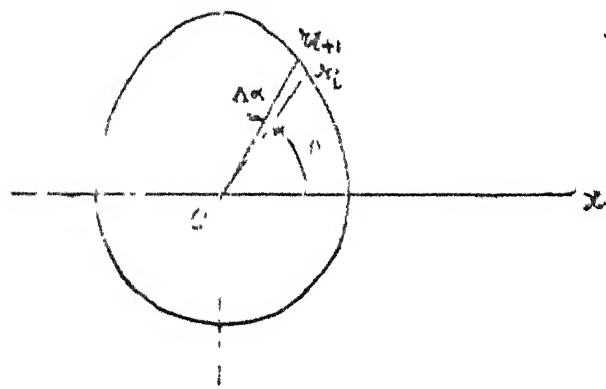


FIG. A-1

Appendix II
Derivation of Cam Stiffness

The derivation of approximate estimate of stiffness of the cam body is given here. The (Fig 2.3, 2.4) shows a cam profile and a tapered beam which approximates the cam profile. This beam has its cross sectional area varying over the length of the beam. Let's say a load P is acting at the tip. Under this load the maximum deflection can be computed using castigliano's theorem [17].

$$\delta = \frac{\partial U}{\partial P} = \int_0^L \frac{P^2 x^2 dx}{2 \cdot E \left[\frac{t}{I_2} (a + \frac{b-a}{L} x)^3 \right] 8} \quad \dots \quad (A21)$$

where δ = deflection under the load P

U = strain energy due to P

L = length of the beam

t = uniform thickness of the cam (beam)

x is measured from the tip towards the support

$$= P \int_0^L \frac{x^2 dx}{E \cdot \frac{t}{I_2} (a + cx)^3 \cdot 8} \quad \dots \quad (A22)$$

where $C = \frac{b-a}{L}$

OR

$$\delta = \frac{P}{\frac{2}{3} \cdot E \cdot t / \frac{1}{C^3} [\ln(\frac{b}{a}) - (1 - \frac{a}{b}) + \frac{1}{2} (1 - \frac{a^2}{b^2})] \dots \dots (A23)}$$

Thus the stiffness K_b from (A23) can be computed to be

$$K_b = \frac{\frac{2}{3} E t}{\frac{1}{C^3} \left[\ln \left(\frac{b}{a} \right) - \left(1 - \frac{a}{b} \right) + \frac{1}{2} \left(1 - \frac{a^2}{b^2} \right) \right]} \dots (A24)$$

This is an approximate estimate of stiffness of an actual cam which will give a feel of the order of magnitude of the value of K_b . K_b is dependent on the dimension, b , and L . These values are to be selected compatibly with the size of cam.

Appendix III

Determination of Eigen-value and Eigen-vector.

The undamped equation of motion given by equation (2.23) is a generalised eigen-value problem, in the form,

$$K \phi = \lambda M \phi \quad \dots \dots \quad (A31)$$

where,

K is a ($n \times n$) stiffness matrix

M is a ($n \times n$) mass matrix

ϕ is a ($m \times n$) modal matrix containing

m no. of eigen vectors corresponding to
 m eigen values.

λ is ($m \times m$) diagonal matrix whose non-zero terms are square of natural frequencies.

matrix

In the present problem the order of λ (i.e., n) in K and M are comparatively small. Hence the modal matrix ϕ may contain all the eigen vectors and equation (A31) can be solved for all eigen values.

There are many methods for solving generalised eigen-value problem (e.g. generalised Jacobi method, Q-Z algorithm etc.). The generalised Jacobi method is suitable

when the order of the problem is small. Thus this method is chosen for solving eq (A31). Besides, it has other advantages [1] like it can handle ill-conditioned matrices, it avoids solution of standard eigen value problem and solves (A31) directly, fast convergence is expected when the off-diagonal elements are small.

The modal matrix ϕ satisfies the M-orthogonality as follows $\phi^T M \phi = I$ - (A32) (A32)

and $\phi^T K \phi = \lambda$ (A33)

where I is an identity matrix (A32) and A33) can be used as a check of the solution.

REFERENCES

- [1] Bathe K-J and Wilson E.L., ' Numerical Methods in Finite Element Analysis', Prentice Hall of India, New Delhi, 1978.
- [2] Barkan, P., ' Calculation of High Speed Valve motion with Flexible Overhead Linkage, ' SAE. Transaction, Vol. 61, 1953, pp. 687-700.
- [3] Beer , Johnston ' Vector Mechanics for Engineers', McGraw Hill Kagakusha Ltd., 1977, pp. 382-387.
- [4] Chen Y. Fan., ' Mechanics and Design of Cam Mechanisms', Pergamon Press, New York, 1982.
- [5] Erdman A.G., Sandor G.N. and Oakberg R.C., ' A General method of kineto-elastodynamic analysis and synthesis of Mechanisms,' Trans. ASME, J. Engg. Ind., Vol. 94, 1972, pp. 1193-1205.
- [6] Erdman A.G. and Sandor G.N., ' KED-a review of the state of the art and trends', Mechanism and Machine Theory, Vol. No. 1, Spring 1972.
- [7] Iman I., Sandor G.N. and Kramer S.N., ' Deflection and Stress analysis in High Speed planer Mechanisms with elastic links.', Trans. ASME, J. Engg. Ind., Vol. 95, 1973, pp.541 - 548.

- [8] Midha A., Eraman, A .G., and Frohrib, D.A., ' Finite element Approach to Mathematical Modelling of High-Speed Elastic Linkage', Mechanism and Machine Theory, Vol.13, 1978, pp. 603-618.
- [9] Nath, P.K. ' Kinetoo-Elastodynamic Analysis of High Speed Mechanism,' Ph.D. dissertation, Dept. of Mechanical Engg., Indian Institute of Technology, Kanpur, March 1976.
- [10] Neubauer A.H. Jr., Cohen R. and Hall A.S. Jr., ' An Analytical study of the Dynamics of an Elastic Linkage,' Trans. ASME, J. Engg. Ind., Vol. 88, No.3, Aug. 1966, pp. 311-317.
- [11] Paul, B., ' Kinematics and Dynamics of Planer Machinery', Prentice-Hall-Inc., New Jersy 07632 - 1979, pp.34-37.
- [12] Rothbart A.H., ' Cams - Design, Dynamics and Accuracy', John Willey and Sons, Inc., London, 1956.
- [13] Rubinstein, M.F., ' Matrix Computer Analysis of Structures', Prentice-Hall Inc., Englewood Cliffs, N.J., 1966.
- [14] Stoddart, D.A., ' Polydyne Cam Design', Machine Design, January 1953 (1) pp.121-135, Feb. 1953 (2) pp.146-154, Mar. 1953(3) pp. 149-164.

- [16] Shigley, J.E., ' Theory of Machines', McGraw Hill Book Co. Ltd., Tokyo, 1961.
- [17] Srinath, L.S., ' Advance Mechanics of Solids', TMH Publishing Co. Limited, New Delhi, 1983, pp.147-148.
- [18] Thompson ' Theory of Vibration with application ', Prentice Hall of India Limited, 1982, pp.25-35.
- [19] Winfrey, R.C., ' Dynamic Analysis of Elastic Link Mechanisms by Reduction of Coordinates', Trans. ASME, J. Engg. for Industry, May 1972, pp. 577-582.
- [20] Winfrey, R.C., Anderson, R.V. Gnilka, C.W., ' Analysis of Elastic Machinery with clearances', ASME Trans. J. Engg. Ind., Aug. 1973, pp. 695-703.
- [21] Winfrey, R.C., ' Elastic link Mechanism Dynamics ', Trans ASME, J. Engg. Ind., Vol 93, 1971, pp.268-272.

87573

DATE SLIP 87573

This book is to be returned on
the date last stamped